




Systematic and morphogeometric analyses of Pachyrukhinae (Mammalia, Hegetotheriidae) from the Huayquerías, Mendoza (Argentina): biostratigraphic and evolutionary implications

Bárbara Vera & Marcos D. Ercoli

To cite this article: Bárbara Vera & Marcos D. Ercoli (2018) Systematic and morphogeometric analyses of Pachyrukhinae (Mammalia, Hegetotheriidae) from the Huayquerías, Mendoza (Argentina): biostratigraphic and evolutionary implications, *Journal of Vertebrate Paleontology*, 38:3, e1473410, DOI: [10.1080/02724634.2018.1473410](https://doi.org/10.1080/02724634.2018.1473410)

To link to this article: <https://doi.org/10.1080/02724634.2018.1473410>

 View supplementary material 

 Published online: 03 Jul 2018.

 Submit your article to this journal 

 View Crossmark data 

SYSTEMATIC AND MORPHOGEOMETRIC ANALYSES OF PACHYRUKHINAE (MAMMALIA, HEGETOTHERIIDAE) FROM THE HUAYQUERÍAS, MENDOZA (ARGENTINA): BIOSTRATIGRAPHIC AND EVOLUTIONARY IMPLICATIONS

BÁRBARA VERA^{1,*} and MARCOS D. ERCOLI²

¹Centro de Investigación Esquel de Montaña y Estepa Patagónica (CIEMEP), CONICET, Roca 780, 9200, Esquel, Chubut, Argentina, barbara.vera@comahue-conicet.gob.ar;

²Instituto de Ecorregiones Andinas (INECOA), Universidad Nacional de Jujuy, CONICET, IdGyM, Av. Bolivia 1661, Y4600GNE, San Salvador de Jujuy, Argentina, marcosdarioercoli@hotmail.com

ABSTRACT—We present new remains of Pachyrukhinae (Hegetotheriidae) from the Huayquerías del Este (Mendoza, Argentina). We identify *Tremacyllus impressus*, proposing *T. subdiminutus* as a synonym and providing new data on postcranial bones for this taxon. *Tremacyllus* specimens from Mendoza reveal a wide and continuous morphological variation that encompasses the morphological differences of species previously considered valid, emphasizing the need for a systematic study focused on all representatives of the genus. We also recognize *Paedotherium typicum*, which shows a combination of features differing from other species of the genus. The large sample allows us to improve the diagnosis for both the genus *Tremacyllus* and the species *T. impressus* and *P. typicum*. Both species coexist in the Huayquerías Formation; *T. impressus* is also present in the Tunuyán Formation, whereas the specimens recognized as *Paedotherium* in this unit were not identifiable at species level. Applying geometric morphometric methods on the dentition, we partially support the taxonomic decisions. We present the first phylogenetic analysis including all the species of *Tremacyllus* and *Paedotherium*, using morphological characters of skull and postcranium. According to our results, *Tremacyllus* is a monophyletic group supported by two synapomorphies, whereas *Paedotherium* is paraphyletic, in agreement with the prior hypothesis. The record of *Paedotherium typicum* presented here extends the biochron of this taxon into the late Miocene, which is relevant for establishing biostratigraphic and paleobiogeographic affinities with other Miocene localities.

SUPPLEMENTAL DATA—Supplemental materials are available for this article for free at www.tandfonline.com/UJVP

Citation for this article: Vera, B., and M. D. Ercoli. 2018. Systematic and morphogeometric analyses of Pachyrukhinae (Mammalia, Hegetotheriidae) from the Huayquerías, Mendoza (Argentina): biostratigraphic and evolutionary implications. *Journal of Vertebrate Paleontology*. DOI: 10.1080/02724634.2018.1473410.

INTRODUCTION

The ‘Huayquerías de Mendoza’ is an extensive area of Neogene continental deposits that crop out in the distal piedmont of the Frontal Andean Range (Folguera and Zárate, 2009). It is located in north-central Mendoza Province (San Carlos Department), at a distance of 100km from Mendoza City (Argentina; Fig. 1). Both its sediments and its fauna have attracted the attention of a number of geologists and paleontologists since the beginning of the 20th century (De Carles, 1911; Rovereto, 1914; Kraglievich, 1934; Rusconi, 1939; Linares, 1981; Marshall et al., 1986; Yrigoyen, 1993, 1994). Two main fossiliferous localities are known in this area, separated by the Meseta Sinclinal del Guadal (Synclinal Plateau): the Huayquerías de San Carlos to the west and the Huayquerías del Este (Eastern Badlands) to the east. In the latter, three geological units were recognized, the Huayquerías (late Miocene), Tunuyán (early Pliocene), and Bajada Grande (upper Pliocene) formations, whereas only the latter two formations were identified in the Huayquerías de San Carlos (De Carles, 1911; Groeber, 1939; Dessanti, 1946; Marshall et al., 1986; Yrigoyen, 1993, 1994).

In particular, the Huayquerías Formation bears a peculiar vertebrate fossil association that was the basis for the Huayquerian SALMA (South America Land Mammal Age; Kraglievich, 1934; Simpson, 1940); the isotopic K/Ar age of 5.8Ma reported by Marshall et al. (1986) at the top of this unit was used to calibrate the Huayquerian and Montehermosan mammal-bearing formations based on the De Carles (1911) collections (Yrigoyen, 1994). In Argentina, Huayquerian assemblages are also recognized in low latitudes such as the Chiquimil (El Jarillal Member) and Andahuala formations, both in Catamarca Province (Riggs and Patterson, 1939; Bonini, 2014; Nasif and Georgieff, 2014); in the Salicas Formation (La Rioja; Brandoni et al., 2012), in San Juan Province (Contreras and Baraldo, 2011); and in the Palo Pintado Formation, in Salta Province (Reguero et al., 2015). At middle latitudes, the vertebrate fauna from the Cerro Azul and Epecuén formations (La Pampa and Buenos Aires provinces) are also attributed to the Huayquerian age (Montalvo and Casadio, 1988; Montalvo et al., 1995; Verzi et al., 1999, 2008; Folguera and Zárate, 2009, 2011).

From the ‘Huayquerías’ area sensu lato, Rovereto (1914) mentioned two taxa of pachyrukhine Hegetotheriidae in the transitional horizon between his ‘Araucan’ and the Hermosan, which was later recognized as the Tunuyán Formation (Yrigoyen, 1994). On the one hand, Rovereto (1914) described *Tremacyllus subdiminutus* based on a palate with the left cheek tooth row and pointed out that it is larger than ‘*T. diminutus*’ (= *T. impressus*; Cerdeño and Bond, 1998, and references therein) from

*Corresponding author.

Color versions of one or more of the figures in the article can be found online at www.tandfonline.com/ujvp.

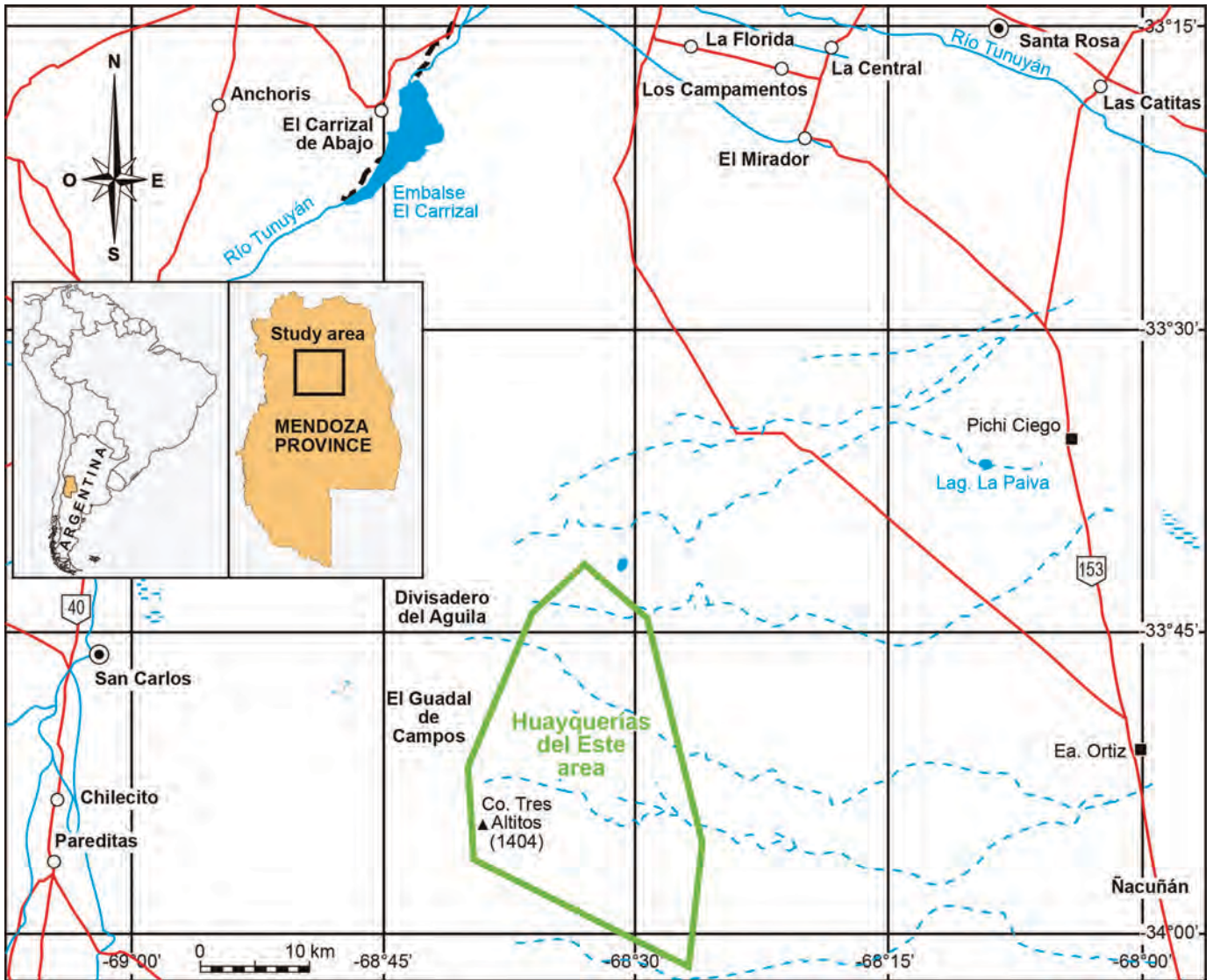


FIGURE 1. Geographic location of the Huayquerías area in the Department of San Carlos, Mendoza Province (Argentina).

Monte Hermoso and smaller than *T. latifrons* Rovereto (1914) from Catamarca. On the other hand, Rovereto (1914) also mentioned the presence of *Pachyrukhos* sp. Ameghino (1885), alluding to its similarity to *P. 'typicus'* Ameghino (1887a) from the Monte Hermoso locality (Buenos Aires Province); however, no description was provided and its specific determination has remained pending since then. Later, the name *Pachyrukhos* was considered synonymous with *Paedotherium* Burmeister, 1888 (Ameghino, 1889), but Kraglievich (1926) considered the two genera to be different taxonomic entities; later, *Pachyrukhos 'typicus'* was partially synonymized with *Paedotherium typicum* and *P. bonaerense* (Cerdeño and Bond, 1998).

Pachyrukhinae is a name coined by Kraglievich (1934) for the small members of the family Hegetotheriidae (Notoungulata), which are characterized by having an inflated tympanic bulla and a diastema between I/1 and P2/p2 and constitute a widely accepted monophyletic group (e.g., Cerdeño and Bond, 1998; Croft and Anaya, 2006; Seoane et al., 2017). Within this subfamily, the post-late Miocene representatives are included in two genera, *Tremacyllus* Ameghino, 1891, and *Paedotherium* Burmeister, 1888 (= *Pachyrukhos* Ameghino, 1885; Ameghino, 1889:439), which are widely distributed in Neogene assemblages

from southern South America. *Paedotherium* currently includes six species: *P. typicum* Ameghino, 1887a, *P. bonaerense* Ameghino, 1887b, *P. minor* Cabrera, 1937, *P. kakai* Reguero, Candela, Galli, Bonini, and Voglino (2015), *P. dolichognathus* (Zetti, 1972a), and the recently revalidated *P. borrelloii* Zetti, 1972b (Ercoli et al., 2017). The record of the genus extends from late Miocene to early Pleistocene? of Argentina and Bolivia (Cerdeño and Bond, 1998; Tomassini et al., 2017, and references therein). *Tremacyllus* is a less represented, although scarcely studied, genus and is infrequently referred to in the literature in comparison with *Paedotherium*; its record is restricted to the late Miocene–early Pliocene from Argentina. Cerdeño and Bond (1998) recognized two valid species of *Tremacyllus*: *T. impressus* (Ameghino, 1888) from the Pampean region (Montehermosan to Marplatán) and *T. incipiens* (= *T. latifrons*) Rovereto (1914) from Catamarca Province. Concerning *T. subdiminutus* from Mendoza, Cerdeño and Bond (1998) indicated that the holotype is very similar to *T. incipiens*, but they did not draw conclusions about its taxonomic validity and recognized that better material is required to establish a synonymy.

In the last five years, several paleontological expeditions to the Huayquerías del Este area have yielded a significant number of

new fossils, increasing the faunal list from seven to more than 20 taxa, including mammals, reptiles, and anurans (Echarri et al., 2013; Forasiepi et al., 2015, 2016; Bonini et al., 2016). More than 130 of these specimens from both the Huayquerías and Tunuyán formations belong to South American native ungulates (Hegetotheriidae, Pachyrukhinae), preliminarily identified as *Tremacyllus* and *Paedotherium* (Echarri et al., 2013; Vera and Ercoli, 2017).

In this contribution, we provide a large sample of new material for this particular group of notoungulates, which allows us to perform a systematic revision, including morphogeometric and phylogenetic analyses of *Tremacyllus* and *Paedotherium*, contribute to the knowledge of the morphological evolution of the Miocene pachyrukhines, and establish paleobiogeographic affinities between the Huayquerías and other Miocene-Pliocene areas.

Geological Settings

The geographic and geological contexts for the Huayquerías and Tunuyán formations, including an integrated stratigraphic column for the former geological unit, were detailed and summarized by Forasiepi et al. (2016). Based on recent field work, Garrido et al. (2017) provided a radiometric date of 5.84 ± 0.41 Ma (Messinian, late Miocene) from a tuff level in the middle-upper part of the Huayquerías Formation and proposed the development of a distal-alluvial depositional system, with which there are associated aeolian and gravelly sandy fluvial systems; the frequent presence of soft-sediment deformation structures probably indicates the recurrence of seismic events towards the final stages of deposition of the Huayquerías Formation. Concerning the Tunuyán Formation, both its age and paleoenvironmental aspects are currently under review (Garrido, unpubl. data).

MATERIALS AND METHODS

The studied specimens were collected during four field seasons (2013–2016), and they are curated at the Vertebrate Paleontology collection of Instituto de Nivología, Glaciología y Ciencias Naturales (IANIGLA-PV), Mendoza (Argentina). For comparisons, we also included the specimens collected by Rovereto and others that are housed in several institutions (see below).

In addition to the qualitative descriptions, we performed geometric morphometric analyses of the upper and lower cheek tooth rows in order to quantify and support the morphological (shape and size) differences described. This kind of dual approach (e.g., the combination of qualitative and morphogeometric analyses) has been shown to be effective in segregating and characterizing taxa through simplified, subtly changing, pachyrukhine cheek tooth structures. We analyzed complete series (P2–M3 and p2–m3), with additional subanalyses of incomplete cheek tooth rows (e.g., P3–M2 and p3–m2), with the objective to include more (although fragmentary) specimens. In order to perform these geometric morphometric analyses, we use the sample, landmark designs, and geometric morphometric methods (e.g., principal component analyses and centroid size analyses) constructed, applied, and explained by Ercoli et al. (2017). In the present study we included *Paedotherium bonaerense*, *P. borrelloi*, *P. typicum*, and *P. minor*, whereas in the case of *Tremacyllus* we considered *T. impressus* and the specimens from Catamarca that were attributed to *T. latifrons*, but no distinction from *T. incipiens* was certainly established (see below). Thus, when alluding to specimens from Catamarca, we refer to all of them as the *T. latifrons*–*T. incipiens* group in the text and in the phylogenetic analyses. The specimens of each taxon considered in the analyses are detailed in Appendices 1–2.

Finally, a phylogenetic analysis was performed using cladistic methodology (TNT 1.1; Goloboff et al., 2008). The morphological data matrix is modified from Cerdeño and Bond (1998), and comprises 10 taxa and 35 morphological characters. We here include,

for the first time, all the species presently recognized in *Paedotherium* and *Tremacyllus* and added discrete skull (12) and postcranial (4) characters (Supplementary Data 1 and 2); for example, character 1 in Cerdeño and Bond (1998) was split into two characters (0 and 15). In particular, characters for the humerus (31) and femur (32) were taken from Elissamburu (2004) and Elissamburu and Vizcaino (2005). All characters were treated as unordered, and maximum parsimony under equal weights was assumed. The strategy of searching consisted of a branch-and-bound search algorithm (implicit enumeration in TNT), which guarantees finding all most parsimonious trees. Support values were calculated using Bremer and Jackknife indices (see Goloboff et al., 2003).

Institutional Abbreviations—**ACM**, Amherst College Museum of Natural History, Amherst, Massachusetts, U.S.A.; **AMNH FM**, American Museum of Natural History, Fossil Mammals Collection, New York, New York, U.S.A.; **IANIGLA-PV**, Colección Paleontología de Vertebrados, Instituto de Nivología, Glaciología y Ciencias Naturales, Mendoza, Argentina; **FMNH**, Field Museum of Natural History, Chicago, Illinois, U.S.A.; **IDGYM**, Instituto de Geología y Minería San Salvador de Jujuy, Argentina; **MACN**, Museo Argentino de Ciencias Naturales, A. Ameghino and **Pv**, Paleontología de Vertebrados collections, Buenos Aires, Argentina; **MHIN UNSL GEO**, Museo de Historia Natural, Universidad de San Luis, San Luis, Argentina; **MLP**, Museo de La Plata, Universidad Nacional de La Plata, La Plata, Argentina; **MMP**, Museo de Mar del Plata, Mar del Plata, Argentina; **MUFyCA**, Museo Universitario Florentino y Carlos Ameghino, Rosario, Argentina; **PVL**, Colección Paleontología de Vertebrados Lillo, Instituto Miguel Lillo, Tucumán, Argentina; **S. Sal. Scar. Paleo**, Museo de San Carlos, Salta, Argentina; **YPM-PPPU**, Yale Peabody Museum, Vertebrate Paleontology Princeton University Collection, New Haven, Connecticut, U.S.A.

Anatomical Abbreviations—**ant p.**, antorbital process; **APD**, anteroposterior diameter; **cub. fc**, cuboid facet; **dl. l.**, distolingual lobe; **ec. fc**, ectal facet; **f**, foramen; **fib. fc**, fibular facet; **gt**, greater tubercle; **H**, height; **hh**, humeral head; **I/i**, upper/lower incisor; **if**, incisive foramina; **L**, length; **M/m**, upper/lower molar; **mst. c**, masseteric crest; **P/p**, upper/lower premolar; **pf**, palatal foramen; **pid**, postincisor depressions; **sus. fc**, sustentacular facet; **TD**, transversal diameter; **W**, width.

RESULTS

Shape Analyses—The morphospace description and patterns of segregation of taxa in the cheek tooth series here analyzed have already been described in detail by Ercoli et al. (2017). In this section, we summarize the main shape changes, especially in the pachyrukhine representatives from Mendoza.

P2–M3—The first three axes of the principal component analysis of P2–M3 explained 65.3% of the total shape changes of the sample (PC1: 41.9%, PC2: 13.8%, PC3: 9.6%; Fig. 2A). There are two principal clusters of species for the first two PCs. A first cluster, located at central and positive values of PC1, is composed of representatives of *Pachyrukhos moyani*, *Paedotherium typicum*, *P. minor*, *Tremacyllus impressus*, and *T. latifrons*–*T. incipiens*, which progressively present a reduction of labial folds on all teeth, a less molarized condition of P3–4, a reduction of the length and size of premolars, an increase in the imbrication and labiomerial projection of the premolars, and an enlargement of the molar series, in which the M3 is smaller than M2 and presents an acute distal projection. It is worth noting that specimens of *Pachyrukhos* tend to differ from the species of *Paedotherium* and *Tremacyllus* by their location at central values of PC1 and negative values of PC2, with more folded labial faces and narrow cheek teeth (Fig. 2A). In turn, this cluster is divided in two groups on PC3, with *Tremacyllus* sp. placed at negative values, due to widening of the cheek teeth, a distal migration of the paracone, reduced labial folds in all cheek teeth, and a

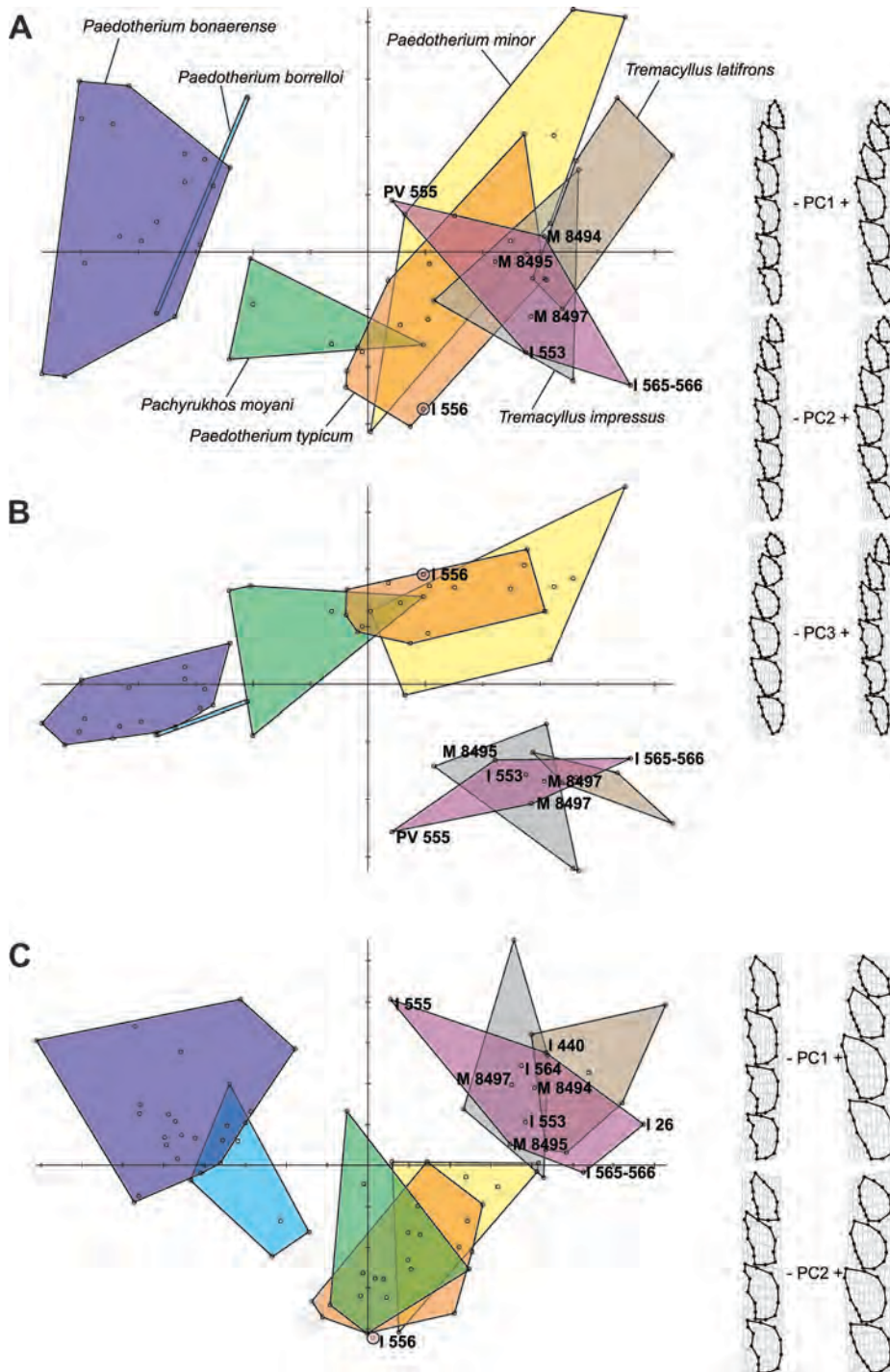


FIGURE 2. Plots of the geometric morphometric analyses of upper cheek teeth. **A**, PC1 versus PC2 of the P2–M3 analysis; **B**, PC1 versus PC3 of the P2–M3 analysis; **C**, PC1 versus PC2 of the P3–M2 analysis. Specimens from Mendoza are labeled. Deformation grids for each extreme of the axes are illustrated.

reduction in imbrication and absence of posterolingual grooves in premolars (Fig. 2B). The second cluster, located at negative values of PC1 is composed of specimens of *Paedotherium borrelloi* and *P. bonaerense*, which display conspicuous labial folds, an enlargement in the length and size of premolars, molarized premolars, and an M3 larger than M2 (Fig. 2A).

The six specimens of *Tremacyllus* from Mendoza included in this analysis are located in the morphospace of *T. latifrons*–*T. incipiens*, *T. impressus*, and adjacent regions (Fig. 2A–B). These specimens reveal a diverse and continuous range of cheek tooth shapes, from square premolars and an M1 that is relatively larger

than M2–3 (e.g., IANIGLA-PV 555) to labiomesially elongated premolars and similarly sized molars. The single representative of *Paedotherium* from Mendoza included in this analysis (e.g., IANIGLA-PV 556) is located within the area of *P. typicum*, and secondarily close to *P. minor* and *Pachyrukhos* (Fig. 2B). This specimen possesses morphological traits present in *P. typicum*, such as well-imbricated premolars with a posterolingual sulcus (moderately excavated in P4), a straight cheek tooth series, and an M3 larger than M2 (see below).

P3–M2—The first two axes of the principal component analysis explained 54.3% of the total shape changes in the

sample (PC1: 39.8%, PC2: 14.5%; Fig. 2C). Despite the large number of representatives for each taxon, the exclusion of P2 and M3 in this analysis resulted in a better separation of taxa compared to the P2–M3 analysis. Three principal clusters of species are clearly defined in the first two PCs, and the segregation of species inside each cluster is also improved (Fig. 2C).

A first cluster, mainly located at positive values of PC1 and PC2, is composed of *Tremacyllus* sp. specimens; a second cluster, mainly located at central values of PC1 and negative values of PC2, is composed of specimens of *Paedotherium minor*, *P. typicum*, and *Pachyrukhos moyani*; and a third cluster, located at negative values of PC1, is composed of specimens of *Paedotherium borrelloii* and *P. bonaerense*. The associated shape changes for each cluster on the first two principal components are the same to those already described in the P2–M3 analysis, with the addition of the segregation of *Tremacyllus* sp. and *Paedotherium bonaerense* toward positive values of PC2, due to the expansion of the lingual face of the premolars and the loss of the posterolingual sulcus (Fig. 2C). As in the P2–M3 analysis, *Pachyrukhos* partially splits from

Paedotherium minor and *P. typicum* toward positive values of PC4, due to the same shape changes as described above.

As occurred in the P2–M3 analysis, the nine specimens of *Tremacyllus* from Mendoza included in this analysis are located in the morphospace of *T. incipiens*, *T. impressus*, and adjacent regions, demonstrating a relatively wide range of shapes (Fig. 2C). The single representative of *Paedotherium* from Mendoza included in this analysis (e.g., IANIGLA-PV 556) is very similar in shape, and is located close to the representatives of *P. typicum*, and secondarily close to *P. minor* and *Pachyrukhos* (Fig. 2C).

p2–m3—The first two axes of the principal component analysis of p2–m3 explained 72.6% of the total shape changes of the sample (PC1: 65.4%, PC2: 7.3%; Fig. 3A). There are four principal clusters of species along the first PC, whereas the remaining axes did not allow major segregations. A first cluster, located at negative values of PC1, is composed of specimens of the two species of *Tremacyllus*, with *T. incipiens* specimens located at more extreme negative values than *T. impressus* specimens. A second cluster, located at central to negative values of PC1, is composed of *Paedotherium typicum* and *P. minor*. A third cluster, located

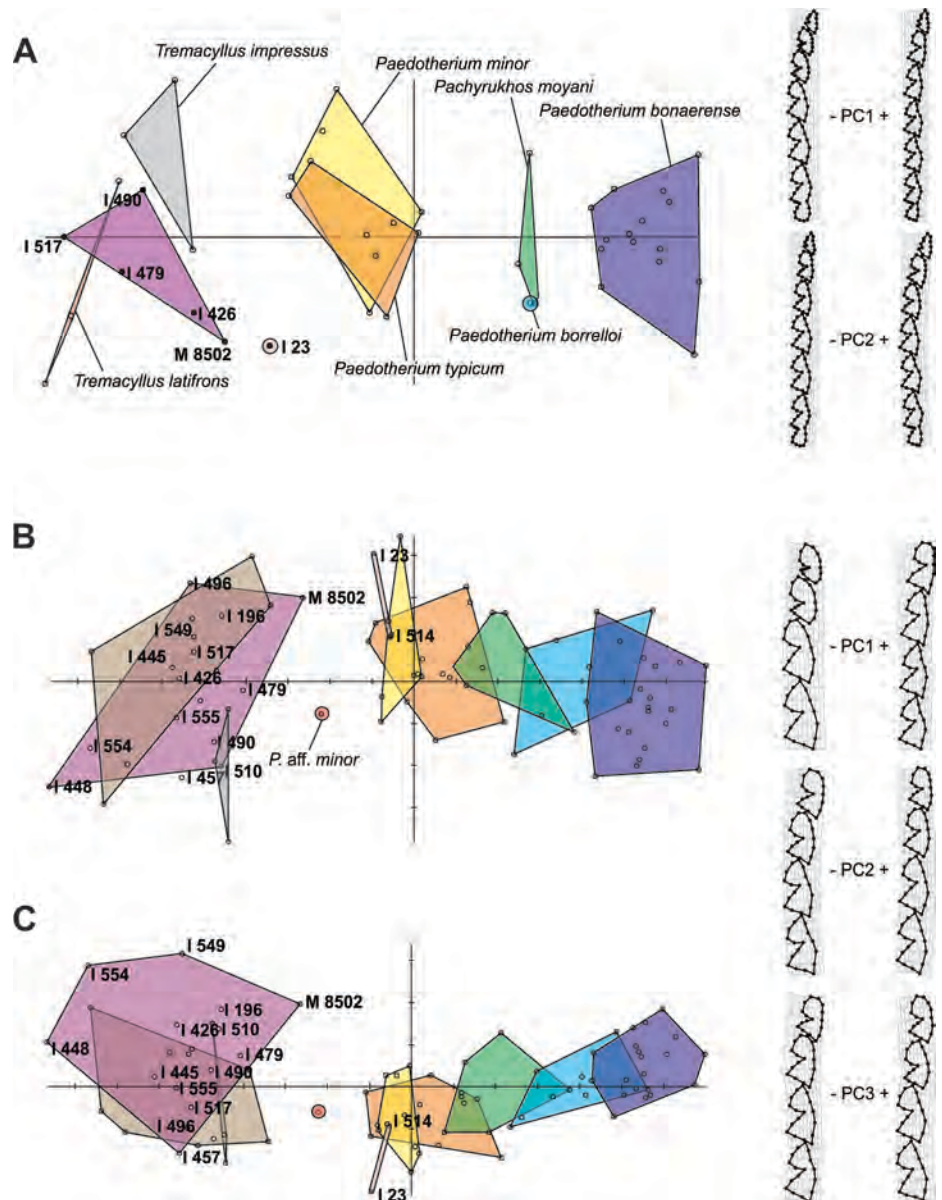


FIGURE 3. Plots of the geometric morphometric analyses of lower cheek teeth. **A**, PC1 versus PC2 of the p2–m3 analysis; **B**, PC1 versus PC2 of the p3–m2 analysis; **C**, PC1 versus PC3 of the p3–m2 analysis. Specimens from Mendoza are labeled. Deformation grids for each extreme of the axes are illustrated.

at positive values of PC1, is composed of *P. borrelloii* and *Pachyrukhos moyani*. Finally, the fourth cluster is located at extreme positive values and is only composed of *P. bonaerense* (Fig. 3A). From the first to the fourth clusters, there is a progressive increase in the size and length of the premolars (in contrast to molars), a reduction of imbrication, and enhancement of molarization of the premolars, i.e., p3 and p4 acquire a less rounded contour of the anterior lobe and an enlarged posterior one. Additionally, the lingual margin of the premolars changes to a less convex shape, and the lingual margin of the molars changes to a markedly sinuous pattern, whereas the third lobe of the m3 acquires a more triangular shape (Fig. 3A).

The five specimens of *Tremacyllus* from Mendoza included in this analysis are located in the morphospace of *T. incipiens*, *T. impressus*, and adjacent regions (Fig. 3A), as occurred in the analyses of the upper cheek teeth (see above). The shape of these specimens varies from an extremely imbricated and short premolar series (e.g., IANIGLA-PV 490, IANIGLA-PV 517) to a moderately imbricated and large premolar series (e.g., MACN-Pv 8502); the shape of the posterior lobes of the premolars (especially p2 and p3) is also variable: from wide (IANIGLA-PV 490) to narrow and reduced (e.g., MACN-Pv 8502, IANIGLA-PV 426); in turn, no major changes are registered in the molar series, independent of the degree of imbrication. The single representative of *Paedotherium* from Mendoza included in this analysis (e.g., IANIGLA-PV 23) is located in an exclusive region of the morphospace, intermediate between the distribution areas of *P. typicum* plus *P. minor* and *Tremacyllus* spp., with a moderately short and barely trilobed p2, and p3 broken but reconstructed as possessing a similar or slightly smaller posterior lobe than anterior lobe, and moderate imbrication and molarization of premolars.

p3–m2—The first three axes of the principal component analysis of the p3–m2 series explained 74.5% of the total shape changes of the sample (PC1: 63.5%, PC2: 6.9%, PC3: 4.1%; Fig. 3B–C). The exclusion of p2 and m3 in this analysis resulted in a better separation of the species grouped in the clusters of the p2–m3 analysis, but a greater overlap between species of different clusters. Thus, there is a more transitional pattern of segregation along PC1, formed by *Tremacyllus incipiens*, *T. impressus*, *Paedotherium* aff. *minor* (see Ercoli et al., 2017), *P. minor*, *P. typicum*, *Pachyrukhos moyani*, *Paedotherium borrelloii*, and *P. bonaerense*, from negative to positive values of this axis (Fig. 3B). The associated shape changes for this gradient-like pattern in the first principal component agree with those already described in the P2–M3 analysis, without major differences.

In this analysis, the large sample (14 specimens) of *Tremacyllus* from Huayquerías resulted in a distribution along a broad area in the morphospace of negative values of PC1, overlapping with many of the *T. incipiens* and *T. impressus* specimens

(Fig. 3B). The diversity of shapes is more clearly represented, registering a wide range of degrees of imbrication and shapes of posterior lobes, and curvatures and imbrication of premolar series along PC1 and PC2, respectively (Fig. 3B). The two representatives of *Paedotherium* from Mendoza included in this analysis (e.g., IANIGLA-PV 23, IANIGLA-PV 514) are located inside the distribution area of *P. typicum* and *P. minor*, with a p3 having a similar or slightly larger anterior lobe than posterior lobe, and moderate imbrication and molarization of premolars, as described in the p2–m3 analysis.

Size Analyses

The range of sizes for each species of pachyrukhine was discussed in detail by Ercoli et al. (2017), who realized that the species present a range of sizes that overlap each other. *Tremacyllus* representatives are typically smaller than *Paedotherium* ones; in the latter genus, *P. minor* and *P. borrelloii* are the smallest species, whereas *P. bonaerense* is the largest. For upper (P3–M2; Fig. 4A) and lower (p3–m2; Fig. 4B) cheek teeth, *Tremacyllus* representatives from Mendoza show centroid size values that are similar to (P3–M2 size) or similar to lower (p3–m2 size) than those of *T. impressus* and the *T. latifrons*–*T. incipiens* group. In both analyses, the centroid size values of the *Tremacyllus* representatives from Mendoza are typically smaller than the smallest species of *Paedotherium* (e.g., *P. borrelloii* and *P. minor*). In turn, the *Paedotherium* representatives from Mendoza display moderate to high centroid size values, matching the lower values of *P. bonaerense* and higher values of *P. borrelloii* and *P. typicum* (p3–m2 size; Fig. 4B) or medium values of *P. typicum* and *P. bonaerense* (P3–M2 size; Fig. 4B).

SYSTEMATIC PALEONTOLOGY

NOTOUNGULATA Roth, 1903
HEGETOTHERIIDAE Ameghino, 1894
PACHYRUKHINAE Kraglievich, 1934
TREMACYLLUS Ameghino, 1891

Type Species—*Tremacyllus impressus* (Ameghino, 1888).

Distribution and Age—Buenos Aires Province (San Andrés, Vorohué, Barranca Lobos, Chapadmalal, and Monte Hermoso formations, as well as Bahía Blanca beds; Cerdeño and Bond, 1998; Deschamps, 2005), San Luis Province (Río Quinto Formation; Prado et al., 1998), Córdoba Province (Tauber et al., 2014), La Pampa Province (Cerro Azul Formation; Sostillo et al., 2012), Catamarca Province (Andalhualá Formation; Rovereto 1914; Zetti, 1972a; Bonini, 2014), La Rioja Province (Salicas Formation; Tauber, 2005), and Mendoza Province (La Huertita

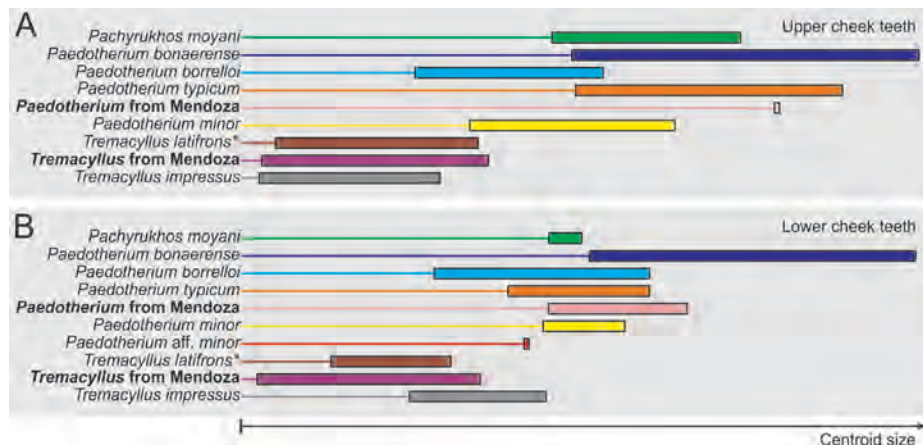


FIGURE 4. Plots of centroid size values for each taxon analyzed. **A**, P3–M2 analysis; **B**, p3–m2 analysis. Specimens from Mendoza are highlighted in bold.

Formation [Garrido et al., 2014] and Huayquerías and Tunuyán formations). Late Miocene–early Pliocene.

Emended Diagnosis—(From Cerdeño and Bond, 1998.) Apomorphies of the taxon: absence of lingual groove on upper premolars; incisive foramina reaching premolar series. Differing from *Paedotherium* and *Pachyrukhos* in smaller size; postincisive depressions reach P2/P3 level; masseteric crest with a stronger anterior process at the m2 level; less-developed antorbital process; presence of a reduced sagittal crest; relatively larger tympanic bulla; more curved P2–M3 rows, with the occlusal plane of premolars at a different angle from that of the molars; DP4 is replaced before M3 erupts; and astragalus with a relatively longer neck. *Tremacyllus* differs from *Paedotherium* by short mandibular symphysis reaching p2 level; mastoid bullae strongly developed beyond condyles; M3 distally narrower and shorter in size than M2; a more developed peroneal tubercle in the calcaneum; and a complete distal keel in metapodials. *Tremacyllus* differs from *Pachyrukhos* in posterodorsally more projected mastoid bullae; asymmetrical and wider astragalar trochlea; and slender calcaneum with relatively longer distal region, smaller sustentaculum and narrower cuboid facet.

Remarks—The genus *Tremacyllus* was erected by Ameghino (1891) to include ‘*Pachyrukhos impressus* Ameghino (1888) from the Pampean region (Buenos Aires and La Pampa provinces). Later, Ameghino (1908) included *Tremacyllus chapadmalensis* and *T. novus*, and Rovereto (1914) described *T. incipiens* and *T. latifrons* from Catamarca, *T. intermedius* from Buenos Aires, and *T. subdiminutus* from Mendoza. Finally, Cerdeño and Bond (1998) retained only two valid species, *T. impressus* (type species) and *T. incipiens*, but their proposed synonymies were inadequately supported (see below). In the context of the present study, although we find some morphological segregation between the two taxa in the geometric morphometric analyses, we encounter difficulty in separating *T. impressus* from *T. incipiens*, taking into account the original diagnosis for these species, which was based on type material. Moreover, these difficulties are enhanced by the fact that the *Tremacyllus* specimens from Mendoza reveal a wide and continuous morphological variation that encompasses the morphological variation of species previously considered valid, given by the morphometric analyses. Taking into account this framework, a synonymy between *T. impressus* and *T. incipiens* is not discarded, but this hypothesis is not adequately supported here because of the need for a systematic study focused on all representatives of the genus, including more and new material. Based on morphological comparison of the large sample of *Tremacyllus* from Mendoza with better-known species of *Tremacyllus* (taking into account type material and some referred specimens) described from other geographic areas (e.g., *Tremacyllus impressus*, *T. incipiens*) and the morphometric results presented above, we recognize *Tremacyllus impressus* in both the Huayquerías and Tunuyán formations. Our proposition makes *T. subdiminutus* a junior synonym of *T. impressus*.

TREMACYLLUS IMPRESSUS (Ameghino, 1888)

(Figs. 5–7)

Pachyrukos impressus Ameghino, 1888:13–14 (original description).

Tremacyllus impressus (Ameghino, 1888): Ameghino, 1891:241.

Tremacyllus subdiminutus Rovereto, 1914:214, fig. 84.

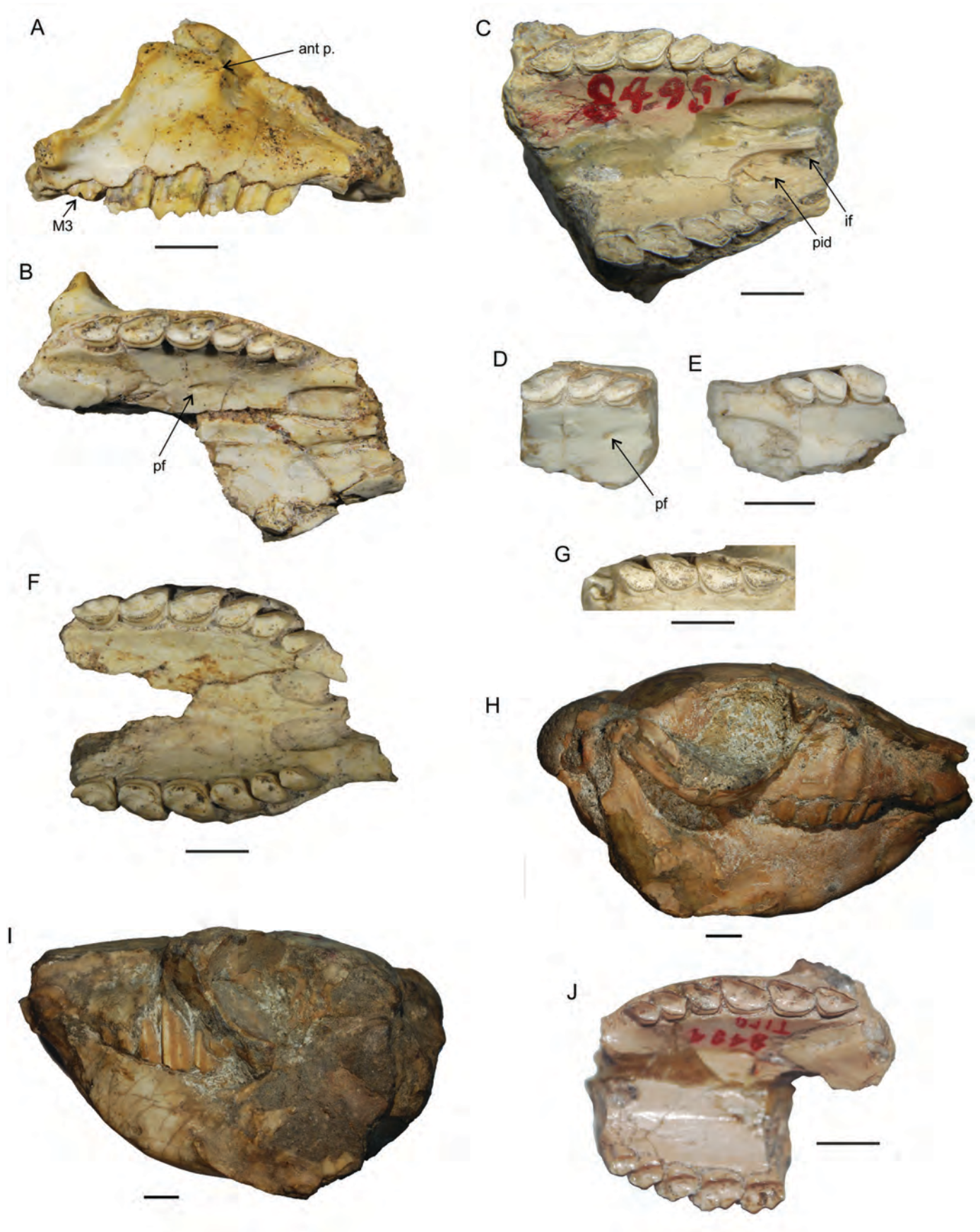
Sintype—MACN-A 1377, partial skull with left P2–M3 and right P3–M3.

Type Locality—Monte Hermoso, Buenos Aires Province.

Distribution and Age—Buenos Aires Province (San Andrés, Vorohué, Barranca Lobos, Chapdmalal, and Monte Hermoso formations; Cerdeño and Bond, 1998) and Mendoza Province

(Huayquerías and Tunuyán formations). Late Miocene–late Pliocene.

Referred Material—Huayquerías Formation. Huayquerías de la Horqueta norte: IANIGLA-PV 91, dentary with p3(broken)–m1; IANIGLA-PV 108, right m3; IANIGLA-PV 418, palate with right and left P2–M3; IANIGLA-PV 419, maxillary fragment with left P3–M2; IANIGLA-PV 420, palate with right P2–M3 and left P3–M2. Huayquerías de la Horqueta sur: IANIGLA-PV 26, palate with right P2–M3 and left broken P2–M3; IANIGLA-PV 27, maxillary fragment with M2–3; IANIGLA-PV 421, hemipalate with right I1, P2–M3; IANIGLA-PV 459, dentary with right p2–4; IANIGLA-PV 473, dentary with right and left m1–2; IANIGLA-PV 475, maxillary fragment with P3–4 and M2–3. Río seco isla grande: IANIGLA-PV 476, dentary with right m1–3; IANIGLA-PV 484, dentary with left m1–3; IANIGLA-PV 497, dentary with right p2–4; IANIGLA-PV 503, dentary with left p2–m3; IANIGLA-PV 550, maxillary fragment with right M1–3; IANIGLA-PV 557, dentary with right i1–2, [right] p2–m3, and left calcaneum; IANIGLA-PV 559, dentary with right p2–m3. Río seco isla chica: IANIGLA-PV 451, dentary with left p2–m3; IANIGLA-PV 478, maxillary fragment with left P4–M1, dentary with left p4–m1; IANIGLA-PV 480, dentary with right m2–3; IANIGLA-PV 485, dentary with right m1–3; IANIGLA-PV 486, dentary fragments with left p4–m3 and right p2–m2; IANIGLA-PV 487, maxillary fragment with left M2–3; IANIGLA-PV 488, maxillary fragment with right M2–3; IANIGLA-PV 496, dentary with right p2–m3; IANIGLA-PV 499, dentary with right p4–m2; IANIGLA-PV 510, dentary with p2–m3; IANIGLA-PV 517, palate with left P3–M3 and right P4–M3 and mandible with right and left p2–m3; IANIGLA-PV 554, palate with right P2–M3 and left P2–M1 and dentary with right and left p2–m3; IANIGLA-PV 555, palate with right and left P2–M3, dentary with left p3–m3, metapodial, right astragalus, distal of right calcaneum, and right navicular. Loma alta norte: IANIGLA-PV 449, palate with right P3–M3 and left P4–M3. Río seco de la última aguada: IANIGLA-PV 539, left trochlea of astragalus, left calcaneum, and left lower molar; IANIGLA-PV 549, mandible with right and left p3–m3. Beautiful canyon: IANIGLA-PV 482, dentary with left p4–m3; IANIGLA-PV 483, dentary with left p2–4; IANIGLA-PV 553, hemipalate with right P2–M3. Tunuyán Formation. Río seco isla grande: IANIGLA-PV 196, dentary with right p3–m2 and proximal of left humerus; IANIGLA-PV 426, mandible with left p2–m3 and right p3–4; IANIGLA-PV 428, dentary with left p2–4; IANIGLA-PV 431, maxillary fragment with right P2–M1; IANIGLA-PV 432, dentary with right p3–m1; IANIGLA-PV 433, dentary with right p4–m1; IANIGLA-PV 436, mandible with left i1–2, [left] p2–m1, and right i1–2, p2; IANIGLA-PV 437, dentary with right m1–3; IANIGLA-PV 440, maxillary fragment with left P2–M3; IANIGLA-PV 441, dentary with left p2–m1; IANIGLA-PV 442, maxillary fragment with left P2–4 and right P3–M1; IANIGLA-PV 443, dentary with right p4–m3; IANIGLA-PV 456, dentary with left m1–3; IANIGLA-PV 457, dentary with right p3–m2; IANIGLA-PV 479, dentary with left i1–c and [left] p2–m3; IANIGLA-PV 490, mandible with right i1–2, [right] p2–m3, left i1–2, and [left] p2; IANIGLA-PV 504, dentary with right p2–m3; IANIGLA-PV 508, dentary with right p2–4; IANIGLA-PV 509, maxillary fragment with left P2–M1 and right P3–M1; IANIGLA-PV 511, maxillary fragment with P3–M1; IANIGLA-PV 551, maxillary fragment with left M1(broken)–3; IANIGLA-PV 560, mandible with right and left i1 and [left] p2–m2; IANIGLA-PV 561, maxillary fragment with left P2–4 and dentary with left m1–3; IANIGLA-PV 562, mandible with right i1, [right] p2–m3, and left i1–2; IANIGLA-PV 565, hemipalate with P2–M3; IANIGLA-PV 567, maxillary fragment P3–M1. Río seco de la última aguada: IANIGLA-PV 427, dentary with right p2–m1; IANIGLA-PV 435, left m3; IANIGLA-PV 465, mandible with left p3–m3 and right p3–m2; IANIGLA-PV 468, dentary with



right m2–3. Bajada del Fuerte: IANIGLA-PV 25, dentary with right p2–m2; IANIGLA-PV 422, dentary with left p3–m1; IANIGLA-PV 445, mandible with left p3–m3 and right p3–m2; IANIGLA-PV 448, dentary with left p2–m2; IANIGLA-PV 452, dentary with right p4–m2. Río seco del agua escondida: IANIGLA-PV 425, dentary with right p3–m1. Unknown location: MACN-Pv 8494, palate with left P2–M3 and right P2–M2; MACN-Pv 8495, palate with right P2–M3 and left P3–M3; MACN-Pv 8496, palate with left P3–M2 and right P4–M2; MACN-Pv 8497, maxillary fragment with right P2–M3; MACN-Pv 8502, dentary with right and left i1–2 and left p2–m3.

Diagnosis—*Tremacyllus impressus* is characterized by imbricated P2/p2–P4/p4; elongated and mesiolingually convex upper cheek teeth; incisive foramina covering the premaxillaries; a wide depression extends variably over the palate to the P2/P3 level; short, steeped, and narrow symphysis; labially bilobed or trilobed p2; variably present distolingual small lobe on m1–2; circular-outlined posterior lobe in m3; posterior-anterior pattern of eruption in premolars; and P4/p4 erupt before M3/m3.

Description and Comparisons

Skull and Upper Dentition—The antorbital foramen is circular, opens anteriorly over the P4, and its lateral border is the small antorbital process (e.g., IANIGLA-PV 553; Fig. 5A). The palate has a very concave surface, and the P2–M3 series forms two convex rows (Fig. 5B). There are two long and narrow incisive foramina covering the surface of the premaxillae from the most anterior border to the premaxillary-palate suture. Beyond the posterior border of each incisor foramen, a wider depression extends variably over the palate to the mesial border of P2 (Fig. 5B), although it can also reach the middle of P3 (e.g., MACN-Pv 8495; Fig. 5C), which indicates a variable feature in the species. Two tiny palatal foramina can be present, variably placed at the P3/P4 or M1 level (e.g., IANIGLA-PV 509; Fig. 5D).

The P2 has a subtriangular outline and an undulating ectoloph due to the convex parastyle and paracone folds (IANIGLA-PV 442; Fig. 5E). The P3–4 differ from P2 in being squarer and labially convex, without differentiated folds. The shape of P3–4 changes among the sample, from square and less imbricated (e.g., IANIGLA-PV 553; Fig. 5B) to more labiomésially elongated and more imbricated with increasing wear (e.g., IANIGLA-PV 440, IANIGLA-PV 555; Fig. 5F). The M1–2 are subrectangular in outline and larger than the premolars (Table 1); they have a straight distal face, convex lingual face, and smoothly undulating ectoloph with paracone, metacone, and metastyle folds (Fig. 5B, F). The M3 differs from M1–2 in having a triangular outline and narrower distal projection (e.g., IANIGLA-PV 517; Fig. 5G). In premolars and molars, the enamel is thin or absent on the mesial and distal faces, and they are lingually covered by a thick layer of cementum (Fig. 5G).

Concerning *T. latifrons* and *T. incipiens* from Catamarca, both holotypes (MACN-Pv 8157 [Fig. 5H] and MACN-Pv 8163 [Fig. 5I], respectively) are articulated and badly preserved skulls that impede observation of the occlusal surface of the teeth and, consequently, establishing proper comparisons between them and other species (e.g., *T. impressus*). In spite of this, Cerdeño and Bond (1998) considered *T. latifrons* a synonym of *T. incipiens* and also established similarity between the holotype of *T. subdiminutus* (MACN-Pv 8494; Fig. 5J) and *T. incipiens* (but see Discussion). Here, we prefer to maintain both species from Catamarca to make

comparisons between them and the specimens from Huayquerías. The comparatively high degree of imbrication and anterolabial expansion of the premolars of specimens attributed to *T. latifrons* (e.g., MACN-Pv 8169) and *T. incipiens* (e.g., MACN-Pv 8163) are also observed in those from Huayquerías (e.g., IANIGLA-PV 26; see more comparisons in Shape Analyses section). Nevertheless, a large sample of the species from Catamarca is required to confirm these comparisons and evaluate the presence of significant morphological differences between *T. incipiens* and other species.

Mandible and Lower Dentition—The symphysis is short, deeply inclined, and markedly narrow, mainly between the i1s in such a way that these teeth form a nearly right angle (e.g., IANIGLA-PV 473, IANIGLA-PV 517; Fig. 6A); its posterior border is at the middle of p2 (e.g., IANIGLA-PV 479, IANIGLA-PV 560; Fig. 6B). The horizontal ramus is very low at the level of p2 ($H = 9.2$ mm), increasing in height backwards ($H = 12$ mm at m1/2 level; Fig. 6C). Labially, there is a foramen at the diastema level and another at the p3/4 or p4/m1 level. The masseteric crest ends in a prominent anterior process, which is stronger than in the species of *Paedotherium* and *Pachyrukhos* (Fig. 6C). (See Table 2 for lower tooth measurements.)

The i1–2 are very procumbent (Fig. 6C). As in *Paedotherium* and *Pachyrukhos*, the i1 is larger than i2 (Table 2) and labiolingually flattened; its mesial face is straight, whereas the distal border is bilobed and wider (Fig. 6D), although it becomes straight with wear (IANIGLA-PV 490). The i2 is a simple tooth in comparison with the i1. A diastema separates i2 from p2 (Fig. 6A, C).

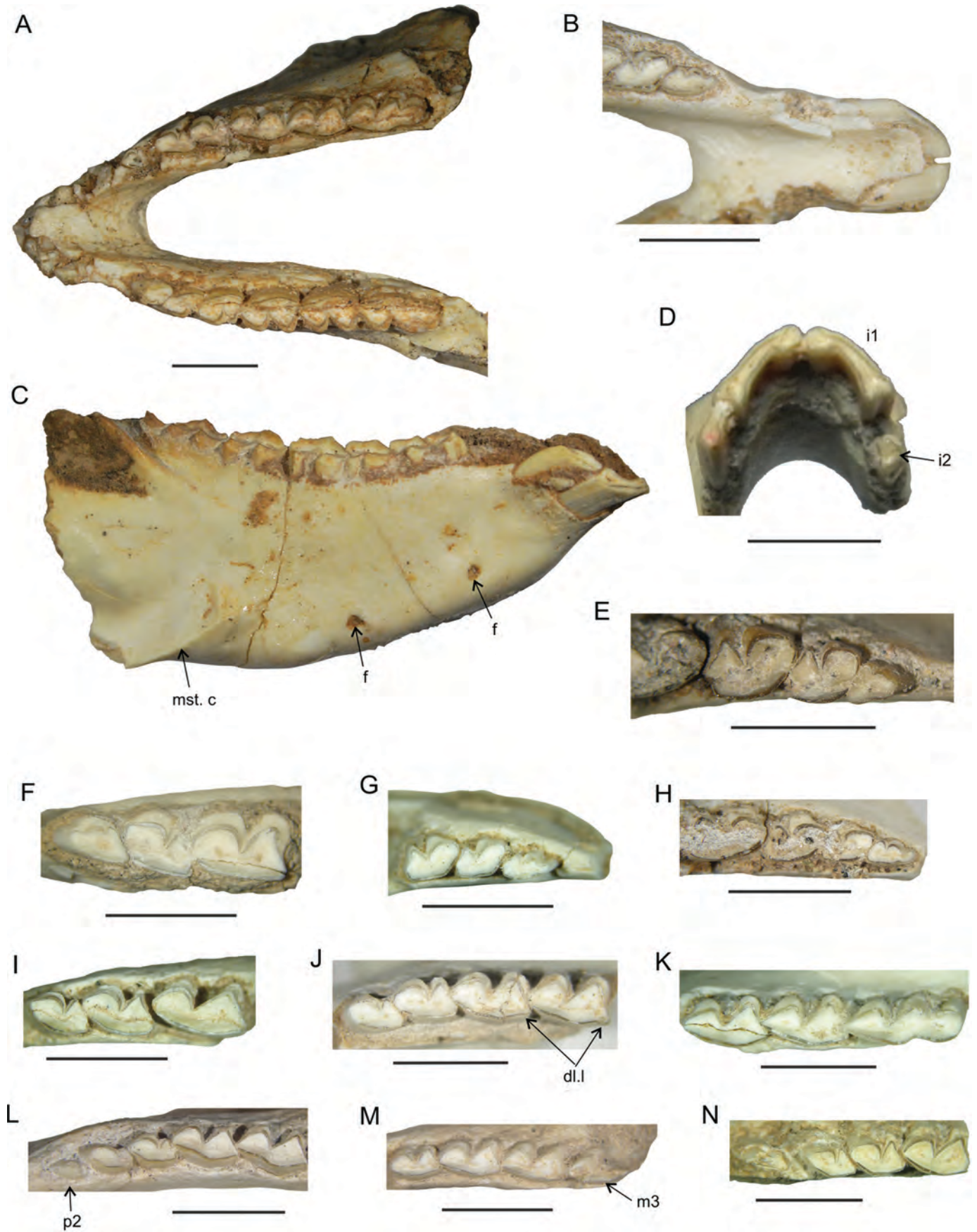
The p2 is the smallest of the premolar series (Table 2) and shows high variability among the specimens that could be explained by the degree of wear. In some cases, the p2 is labially bilobed, with a smoothly concave lingual face; the trigonid and talonid are subtriangular, but the former is longer, narrower, and mesially pointed, whereas the talonid is wider and shorter (e.g., IANIGLA-PV 479, IANIGLA-PV 517, MACN-Pv 8502; Fig. 6A, E). In other specimens the p2 is labially trilobed, with two labial sulci separating a small and forwardly extended mesial lobe from a central lobe (trigonid), and a wider distal lobe (talonid); the lingual face is undulated, with a smooth concavity in the mesial part (e.g., IANIGLA-PV 428, IANIGLA-PV 459, IANIGLA-PV 490, IANIGLA-PV 503; Fig. 6F–H). In very lightly worn p2 (Fig. 6G–H), the mesial lobe is well separated from the central lobe, but with increasing wear both lobes become less defined (e.g., IANIGLA-PV 459; Fig. 6F).

The p3–4 differ from p2 because they have a subsquare trigonid with a well-developed mesial face, differing from the reduced and labially convex trigonid in p2; the talonid is triangular and smaller than the trigonid (Fig. 6F). The premolars are strongly imbricated; the p4 covers the middle lingual part of the distal face of p3, and p3 covers the distal face of p2. The enamel is absent in the mesial face (Fig. 6I).

The m1–2 are similar to each other, differing from the premolars in having a triangular trigonid and a larger talonid that is wider than the trigonid (Fig. 6A, Table 2). The m1 contacts p4 on the labial aspect of its distal corner, and similar contact occurs between m2 and m3 (Fig. 6H, J). In m1–2, there is a very small lobe in the distolingual corner that is variably present depending on the degree of wear of the molars (Fig. 6J).

The m3 is the longest tooth of the molar series (Table 2), labially trilobed and lingually bilobed (Fig. 6A, K); labially, it has an anterior deep sulcus that separates the trigonid from the talonid, and a shallower sulcus between the talonid and the posterior

←FIGURE 5. **A–G**, *Tremacyllus impressus* from Mendoza. **A–B**, IANIGLA-PV 553, hemipalate with right P2–M3, in lateral (**A**) and occlusal (**B**) views; **C**, MACN-Pv 8495, palate with right P2–M3 and left P3–M3, in occlusal view; **D**, IANIGLA-PV 509, maxillary fragment with right P3–M1, in occlusal view; **E**, IANIGLA-PV 442, left P2–4; **F**, IANIGLA-PV 555, palate with right and left P2–M3, in occlusal view; **G**, IANIGLA-PV 517, left P3–M3, in occlusal view. **H**, *Tremacyllus latifrons* (holotype), MACN-Pv 8157, articulated skull. **I**, *Tremacyllus incipiens* (holotype), MACN-Pv 8163, articulated skull. **J**, *Tremacyllus subdiminutus* (holotype), MACN-Pv 8494, palate with left P2–M3 and right P2–M2. Scale bars equal 5 mm.



lobe, which is circular in outline, differing from the labially triangular trigonid and talonid; the lingual face is smoothly convex below the trigonid-talonid and with a marked concavity below the talonid–posterior lobe contact (Fig. 6K). The m3 also differs from m1–2 in having a narrower talonid. The m3 contacts the labial aspect of the distal corner of m2; the enamel is very thin in the distal face of the posterior lobe (Fig. 6K). A layer of cementum covers the labial faces of the lower premolars and molars, in contrast to the upper teeth.

Some differences are observed when comparing the type material of the species of *Tremacyllus*. For instance, MACN-Pv 2434 (holotype of *T. intermedius*) and MACN-Pv 1673 (holotype of *T. diminutus*) have a longer symphysis, p3 similar to p4, which both have a squarer trigonid (with straighter faces) and a shorter talonid. In MACN-Pv 8502 (cataloged as *T. subdiminutus*), the p3 is relatively smaller than p4 and both premolars have a mesiolabially convex trigonid. However, these differences are here considered individual variation in large referred samples, such as those from Huayquerías.

Pattern of Eruption—IANIGLA-PV 554 (Fig. 6L) displays P2/p2–P3/p3 in the process of eruption, with P2/p2 lower in the bone than P3/p3, indicating that P2/p2 are the last teeth to erupt. This pattern is also observed in other notoungulates, such as the Casamayoran Notopithecidae (Vera and Cerdeño, 2014; Vera, 2016) and *Paedotherium* sp. from La Pampa (Cerdeño et al., 2017). In turn, IANIGLA-PV 553 (Fig. 5A–B) has an M3 that is not fully erupted in comparison with completely erupted P3–4; this means that DP4 is replaced before M3 erupts, a feature observed in some notopithecids (Vera, 2016), but differing from *Paedotherium* (Cerdeño et al., 2017) and *Pachyrukhos moyani* (see Vera, 2016). In addition, the specimen IANIGLA-PV 443 (Fig. 6M) shows that the p4 is present when m3 is still emerging (p4 erupts before m3), corroborating a similar condition as described for upper teeth.

In summary, many characters described here were traditionally considered to differentiate *T. impressus*, *T. latifrons*, and *T. subdiminutus* (Ameghino, 1891; Rovereto, 1914; Cerdeño and Bond, 1998), such as the extension of the postincisive depressions, length of symphysis, concavity of palate, shape and imbrication of cheek teeth, and size. The large sample from Mendoza enables us to observe a wide and continuous variability of these traits among specimens, apparently covering diverse configurations previously considered diagnostic of the different species of *Tremacyllus*, including extremes and transitional forms. For instance, MACN-Pv 8502 (cataloged as *Tremacyllus subdiminutus*) differs from IANIGLA-PV 517 in having a longer symphysis and concave distal face on p4 and m2; IANIGLA-PV 445 also has a concave distal face in p3–m2 and an undulating mesial face in p3–4, whereas IANIGLA-PV 427 has a talonid that is wider than the trigonid (Fig. 6N). IANIGLA-PV 503 differs from IANIGLA-PV 422 in having a convex lingual face of p3–4 and m1, whereas in IANIGLA-PV 422 the lingual face is straighter. This variability is here interpreted as intraspecific variation, possibly related to different ontogenetic stages (e.g., age of the individual), stage of wear, or even preservation, which could explain the shape changes of the cheek teeth. However, this hypothesis should be tested with larger samples of *T. latifrons* and *T. incipiens* that would allow us to evaluate the validity of the latter two taxa.

Postcranium

Humerus—IANIGLA-PV 196 is a lot including a proximal fragment of humerus and a dentary. The proximal epiphysis of the humerus is poorly preserved, but it is characterized by its well-developed greater tubercle (Fig. 7A), higher than the humeral head and close to it; this feature is shared with *Paedotherium bonaerense*, and different from *P. typicum* and *Pachyrukhos moyani*, which have a conspicuous greater tubercle well separated from the head (Sinclair, 1909; Elissamburu and Viscaino, 2005). IANIGLA-PV 555 also includes a very fragmented proximal epiphysis of the humerus, which is similar to IANIGLA-PV 196.

Astragalus—IANIGLA-PV 555 is the most complete astragalus ($L = 9.0$ mm), associated with upper or lower dentitions here recognized as *Tremacyllus impressus* (Fig. 7B–E). It has a barely asymmetrical and concave trochlea ($APD = 4.3$ mm; $TD = 4.0$ mm), with both sides well developed and parallel (Fig. 7B); the lateral side is higher and anteroposteriorly wider than the medial one; no superior foramen is observed. The fibular facet is semilunar in shape, very narrow proximally and wider distally (Fig. 7D). The cuboid facet (3.3 mm \times 3.0 mm) is ball-shaped in distal view, separated from the sustentacular facet, and well expanded over the lateral side of the neck. The sustentacular facet is smoothly convex, quite rectangular in outline, and parallel to the vertical axis of the trochlea (Fig. 7C); medially, a wide and shallow interarticular sulcus (sensu Cifelli, 1983) separates this facet from the ectal facet (Fig. 7C); there is no contact with the cuboid facet. The ectal facet is concave, kidney-shaped, and proximodistally well extended; its distal extreme is narrower than the proximal side and laterally well protruded (Fig. 7C–D). The neck is long, but shorter than the height of the trochlea. *Paedotherium bonaerense* (e.g., MLP 99-X-2-1) and *P. typicum* (e.g., MACN-Pv 6436) have a deeper trochlea, shorter neck, wider sustentacular and ectal facets, and laterally more expanded astragalar head. However, *Tremacyllus* and *Paedotherium* share an asymmetrical trochlea. *Pachyrukhos moyani* (e.g., AMNH FM 9481) has a more symmetrical and narrow trochlea that has a more concave surface, and a shorter neck.

Calcaneum—IANIGLA-PV 539 includes a calcaneum associated with a broken astragalar trochlea and a lower molar. The calcaneum is rather well preserved ($L = 15.22$ mm), but its ectal facet is broken (Fig. 7F–G). The sustentaculum is slender and not so laterally extended as in other typotheres (e.g., *Pachyrukhos*; AMNH FM 9481); its facet is subcircular and slightly concave. The ectal facet is observed in IANIGLA-PV 555 (Fig. 7H–I); it is convex and boomerang-shaped, with its distal border wider than the proximal one (Fig. 7H). The cuboid facet (5.6 mm \times 2.5 mm) is narrow and lateromedially very steep (Fig. 7I). As in the Santacrucian hegetotheriids (Sinclair, 1909), there is a navicular-calcaneum contact in *Tremacyllus*. IANIGLA-PV 557 includes a distal fragment of calcaneum (associated with a left dentary), comparable to IANIGLA-PV 539. No noteworthy differences are observed with respect to *Paedotherium* sp. (MACN-Pv 17025 from Miramar, Chapadmalalan); both share a well-developed distal tubercle (peroneal tubercle in Cifelli, 1983) and a short tuber relative to the distal region. In comparison with *Pachyrukhos* (AMNH FM 9481), the calcaneum of *Tremacyllus impressus* is slender, has a longer distal region than tuber, smaller sustentaculum, and narrower cuboid facet.

←FIGURE 6. *Tremacyllus impressus* from Mendoza. **A**, IANIGLA-PV 517, mandible with right and left p2–m3, in occlusal view; **B**, IANIGLA-PV 560, mandible with left i1, [left] p2–4, and right i1, in occlusal view; **C–D**, IANIGLA-PV 490, mandible with right i1–2, [right] p2–m3, left i1–2, and [left] p2, in lateral view (**C**) and detail of incisors (**D**); **E**, IANIGLA-PV 479, dentary with left p2–m1; **F**, IANIGLA-PV 459, dentary with right p2–4; **G**, IANIGLA-PV 428, dentary with left p2–4; **H**, IANIGLA-PV 503, dentary with left p2–m1; **I**, IANIGLA-PV 425, dentary with right p3–m1; **J**, IANIGLA-PV 457, dentary with right p3–m2; **K**, IANIGLA-PV 437, dentary with right m1–3; **L**, IANIGLA-PV 554, dentary with right p2–m2; **M**, IANIGLA-PV 443, dentary with right p4–m3; **N**, IANIGLA-PV 427, dentary with right p2–m1. Scale bars equal 5 mm.

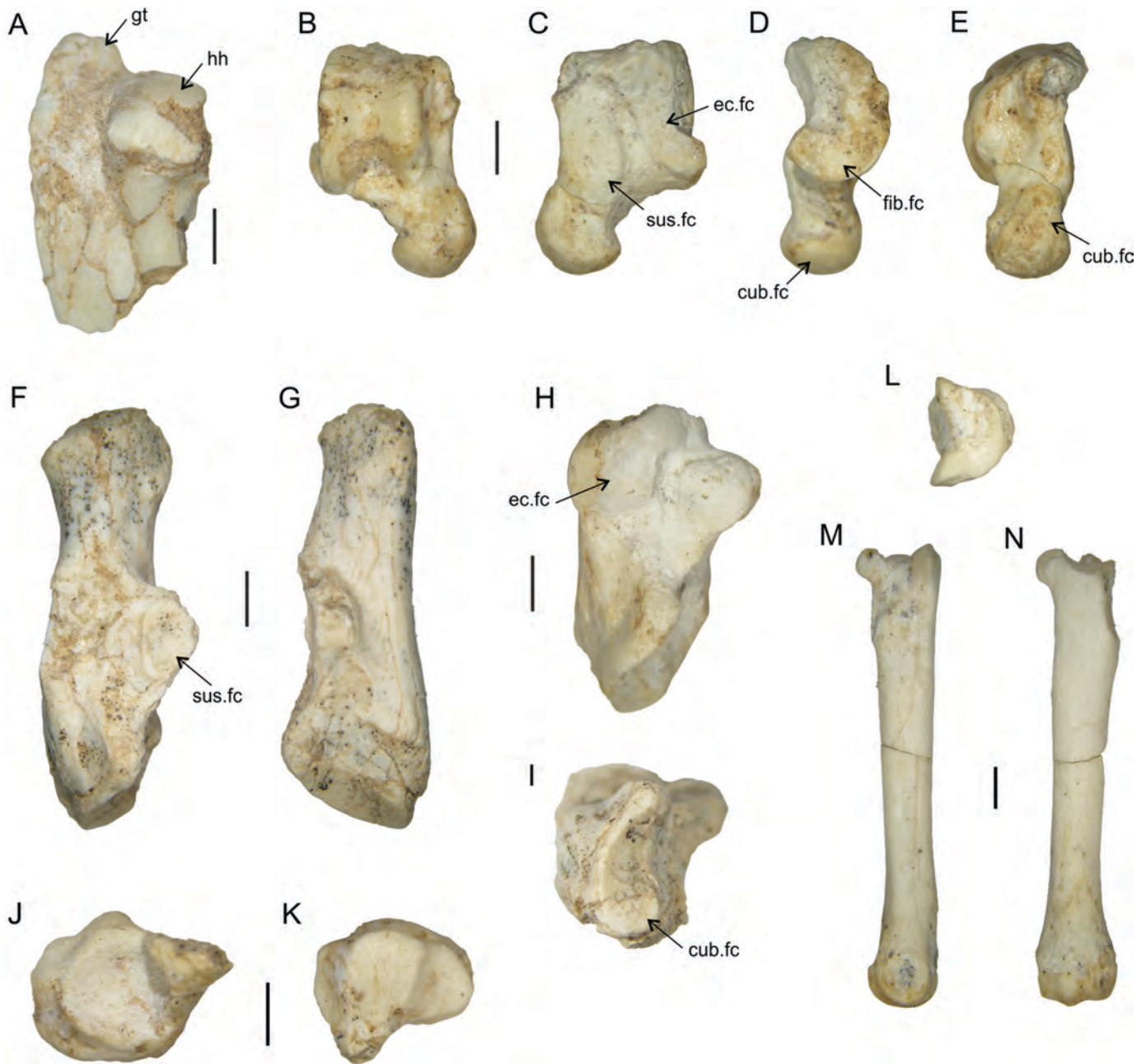


FIGURE 7. Postcranial bones of *Tremacyllus impressus* from Mendoza. **A**, IANIGLA-PV 196, proximal of left humerus; **B–E**, IANIGLA-PV 555, right astragalus, in dorsal (**A**), ventral (**B**), medial (**C**), and lateral (**D**) views; **F–G**, IANIGLA-PV 539, left calcaneum. **H–I**, IANIGLA-PV 555, **H–I**, medial and distal views of right calcaneum; **J–K**, right navicular, in proximal (**J**) and distal (**K**) views; **L–N**, right Mt II, in proximal (**L**), medial (**M**), and dorsal (**N**) views. Scale bars equal 5 mm.

Tarsal Bones and Metapodials—Besides an astragalus and distal part of calcaneum, IANIGLA-PV 555 includes a navicular and a metapodial. The navicular (Fig. 7J–K), which articulates with the astragalus of the same lot, is flat and circular in contour (TD = 4.7 mm; APD = 4.7 mm). It has a circular and mildly concave proximal surface for the astragalus (Fig. 7J); there is a posteriorly well-developed tuberosity. Distally, there are two facets for the cuneiform bones, which are separated by a crest at an acute angle, the lateral facet is fan-shaped and has a flat surface, whereas the medial facet (for the entocuneiform) is a bit larger, concave and subcircular in outline. Laterally, the facet for the cuboid is a small, smoothly convex and wedge-shaped surface (Fig. 7K). With respect to other

pachyrukhines, some general and subtle differences can be mentioned, such as the navicular ACM 1609 attributed to *Paedotherium 'typicus'* from Monte Hermoso, which differs from IANIGLA-PV 555 in being anteroposteriorly elongated and laterally compressed, conferring an ellipsoidal contour to the proximal surface; the distolateral facet is concavoconvex and wedge-shaped, whereas the distomedial facet for the entocuneiform is a somewhat concave and irregular in shape; both facets are in the same plane and separated by a narrow and thin crest, differing from the marked angular separation in *Tremacyllus* (Fig. 7K).

The metapodial (L = 22.0 mm) is here interpreted as a right metatarsal (Mt) II (Fig. 7L–N), comparable in size to the Mt IV

TABLE 1. Upper teeth dimensions (in mm) of Pachyrukhinae.

Taxon	I1		P2		P3		P4		M1		M2		M3	
	AP	T	AP	T	AP	T	AP	T	AP	T	AP	T	AP	T
<i>Tremacyllus impressus</i>														
IANIGLA-PV 26			(2.1)	(1.7)	2.5	2.1	3.3	2.4	4.3	2.7	4.2	2.8	3.8	3.0
IANIGLA-PV 27											4.2	3.3	3.9	2.7
IANIGLA-PV 418			—	1.9	2.6	1.9	3.0	2.5	3.7	3.0	3.8	2.9	3.5	2.5
IANIGLA-PV 419					3.0	2.4	—	2.6	4.2	3.0	4.5	3.3		
IANIGLA-PV 420			2.2	1.6	2.5	2.0	3.0	2.3	3.9	3.3	3.9	3.1	3.7	2.6
IANIGLA-PV 421	5.8	—	—	—	1.5	2.2	—	—	—	—	3.2	2.6	3.3	2.2
IANIGLA-PV 431			1.9	1.5	2.5	2.0	2.8	2.3	3.7	2.4				
IANIGLA-PV 440			2.1	1.8	2.4	1.8	2.7	1.9	3.6	2.4	3.1	2.2		
IANIGLA-PV 442			2.4	1.9	2.6	2.3	3.1	2.5						
IANIGLA-PV 475					2.3	2.1	2.9	2.6						
IANIGLA-PV 478							2.9	2.0	3.7	2.7				
IANIGLA-PV 487											2.9	2.5	3.2	1.8
IANIGLA-PV 488											3.3	2.8	3.3	2.4
IANIGLA PV 509					2.4	2.0	3.0	2.1	3.8	2.6				
IANIGLA-PV 511					2.7	2.3	2.8	2.0	3.9	2.5				
IANIGLA-PV 517							3.0	2.6	3.8	3.1	3.4	2.9	3.5	2.5
IANIGLA-PV 550											3.9	2.8	3.8	2.6
IANIGLA-PV 553			2.5	1.7	2.8	2.0	3.0	2.2	4.1	2.6	4.0	2.8	4.0	2.4
IANIGLA-PV 554			1.5	1.7	2.2	1.8	2.4	2.1	3.4	2.4	3.8	2.6	3.2	2.2
IANIGLA-PV 555			2.3	1.7	2.6	2.1	3.1	2.6	3.9	2.9	3.9	3.0	3.8	2.6
IANIGLA-PV 561			2.1	1.8	2.5	2.4	2.8	2.4						
IANIGLA-PV 565			2.1	1.9	2.5	2.2	2.9	2.5	3.9	2.9	3.9	2.7	4.1	2.5
IANIGLA-PV 567					—	2.1	2.9	2.4	3.9	2.8				
MACN-Pv 8494			2.1	1.9	2.6	2.3	3.0	2.4	4.0	2.7	3.7	2.7	3.6	2.3
MACN-Pv 8495			2.7	2.0	3.0	2.1	3.4	2.5	4.3	3.0	3.7	2.8	—	2.2
MACN-Pv 2434	6.3	1.4	2.5	2.0	2.9	2.3	3.4	2.6	3.8	3.0	3.6	2.9	4.0	2.8
MACN-Pv 2913			2.2	1.8	2.5	2.3	3.0	2.5	3.8	2.9	3.7	2.8	3.8	2.5
MACN-Pv 8169 (<i>Tremacyllus latifrons</i>)			2.5	2.1	3.1	2.8	3.6	2.9	4.3	3.0	3.9	3.0	3.8	2.5
MACN-Pv 1672 (<i>Pachyrukhos diminutus</i>)			2.2	1.7	2.5	2.1	2.8	2.3	3.5	2.5				
<i>Paedotherium typicum</i>														
IANIGLA-PV 469			3.2	2.5	3.5	2.5								
IANIGLA-PV 507											4.8	3.0	5.7	2.9
IANIGLA-PV 556	8.9	1.4	3.3	2.4	—	2.8	4.7	3.0	5.2	3.2	4.9	3.3	5.5	2.9
MACN-PV 8516							3.7	2.5	4.1	2.9	4.2	2.7	4.5	2.4
MACN-PV 8519					2.7	2.3	3.1	3.1	3.9	3.1				
MLP 12-1782			2.7	2.4	3.7	2.4	4.3	2.7	4.7	3.0	4.8	3.0	5.2	2.8
<i>Paedotherium bonaerense</i> *			3.4	2.4	4.6	2.9	4.8	3.1	4.7	3.2	4.4	3.1	4.9	2.8
MLP 57-X-10-88 (holotype <i>P. borrelloii</i>)	7.4	1.5	2.6	2.0	3.7	2.4	4.0	2.6	4.2	2.7	3.8	2.6	4.4	2.3
MLP 29-IX-1-116 (holotype <i>P. minor</i>)	6.6	—	2.5	2.1	3.4	2.6	3.6	2.7	4.4	2.8	3.9	2.7	4.4	2.5
YPM-VPPU 015369 <i>Pachyrukhos moyani</i>	6.4	1.9	3.2	2.1	3.4	2.7	4.2	2.8	4.4	3.0	4.2	2.8	4.3	2.5

*Mean values taken from Cerdeño and Bond (1998).
—, missing data; approximate values in parentheses.

of *Interatherium* (Sinclair, 1909:65); it is a slender bone with a circular diaphysis. The proximal epiphysis has a convex medial edge and concave lateral edge, acquiring a semilunate contour (Fig. 7L); its articular surface for the cuneiform is smoothly concave and narrows anteroposteriorly; its most anterior and posterior borders extend proximolaterally and form two ball-shaped tuberosities for the Mt III; both tuberosities have circular facets extended on the lateral face that are separated by a concave area (Fig. 7M). A well-developed keel is present on the distal epiphysis (Fig. 7N), but it is anteroposteriorly less developed than in *Paedotherium* (e.g., MLP 99-X-2-1). Concerning this character, Cerdeño and Bond (1998) included the presence of a marked distal keel in metacarpals II to IV as diagnostic for *Paedotherium* and differing from *Pachyrukhos*, although they did not mention the presence of a keel in the metatarsals. Nevertheless, Kraglievich (1926) recognized the presence of a distal keel over the dorsal region of the medial metacarpals and metatarsals as a diagnostic feature of *Paedotherium*, differing from *Pachyrukhos*, in which the distal keel is more developed on the ventral surface (AMNH FM 9481; Sinclair, 1909). The morphology of *Tremacyllus impressus* is here described as intermediate between these two taxa, having a complete but less-developed keel.

PAEDOTHERIUM TYPICUM (Ameghino, 1887a)

(Fig. 8)

Pachyrukos typicus Ameghino, 1887a:15 (original description).
Paedotherium typicum (Ameghino, 1887a): Ameghino, 1889; Kraglievich, 1926:57.

Lectotype—MLP 12-1782, incomplete skull with right P2-M3, and mandible with right i1-2, [right] p2-m3, and left p3-m3; same individual.

Type Locality—Monte Hermoso, Buenos Aires Province.

Distribution and Age—Buenos Aires Province (Chapdmal and Monte Hermoso formations; Cerdeño and Bond, 1998), San Luis Province (Río Quinto Formation; Prado et al., 1998), and Mendoza Province (Huayquerías Formation). Late Miocene-late Pliocene.

Remarks—Rovereto (1914) recognized the presence of *Pachyrukhos* sp. in the Huayquerías area, but he did not provide any illustrations or collection numbers for the material. In Rovereto's collection at MACN, we identify three specimens cataloged as *Pachyrukos* from the 'Huayquerías de Mendoza':

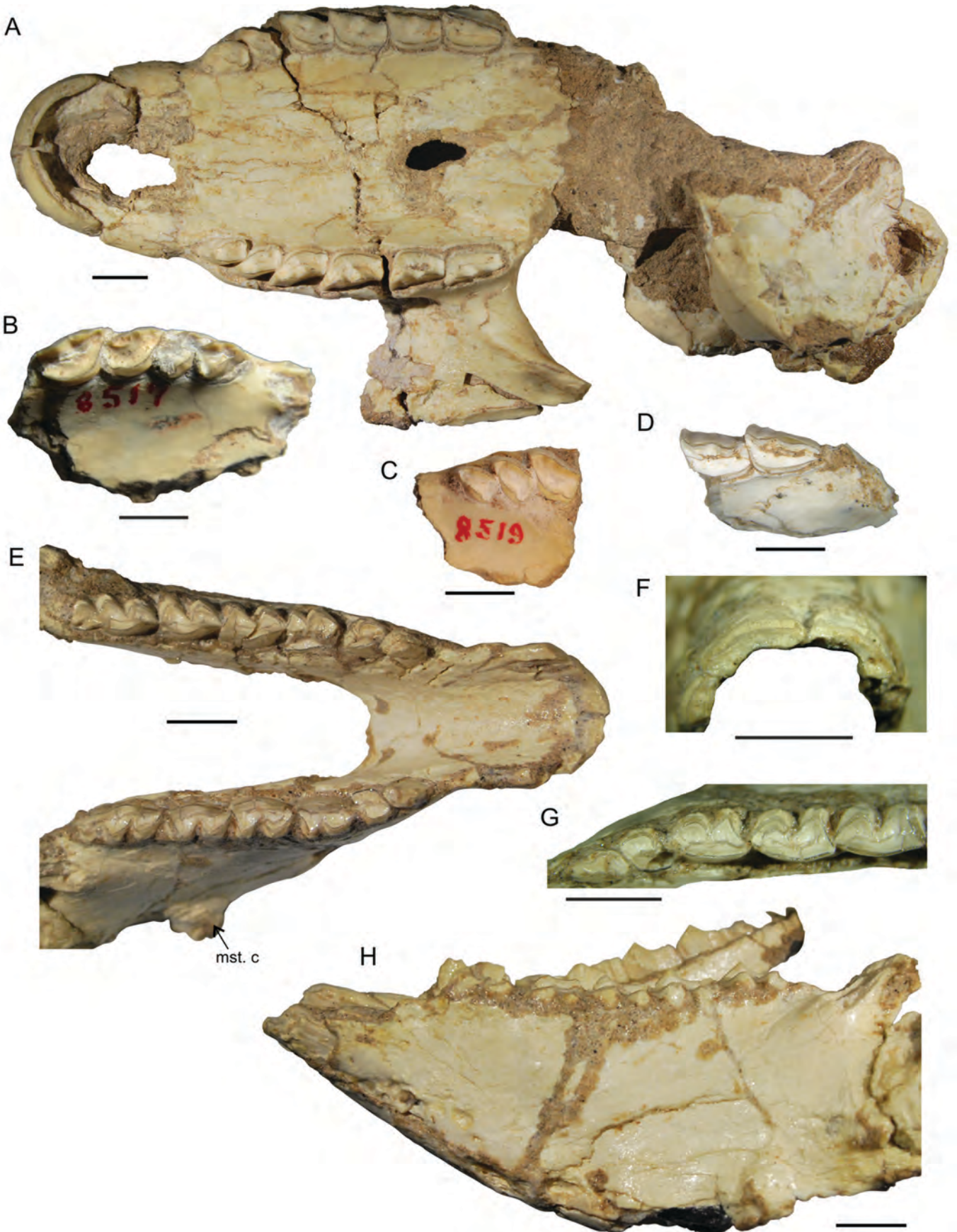
TABLE 2. Lower teeth dimensions (in mm) of Pachyrukhinae.

Taxon	i1		i2		p2		p3		p4		m1		m2		m3	
	AP	T	AP	T	AP	T	AP	T	AP	T	AP	T	AP	T	AP	T
<i>Tremacyllus impressus</i>																
IANIGLA-PV 25					1.7	1.1	2.2	1.7	2.7	1.9	3.2	2.0	3.6	2.1		
IANIGLA-PV 91									2.6	1.9	3.4	2.2				
IANIGLA-PV 108															4.3	1.3
IANIGLA-PV 196							2.4	1.7	2.7	1.9	3.7	2.1	3.9	2.3		
IANIGLA-PV 422							2.3	1.8	2.8	2.0	3.0	2.3				
IANIGLA-PV 425							2.3	1.5	2.9	1.8	3.9	2.0				
IANIGLA-PV 426					1.8	1.1	2.2	1.6	2.6	1.8	3.2	2.1	3.3	2.1	4.4	2.0
IANIGLA-PV 427							2.5	1.4	2.7	1.6	3.4	2.1				
IANIGLA-PV 428					1.7	1.0	1.9	1.5	2.0	1.6						
IANIGLA-PV 432							2.4	1.6	2.7	1.6	3.4	2.0				
IANIGLA-PV 433									2.6	1.8	3.4					
IANIGLA-PV 435															5.1	2.0
IANIGLA-PV 436					1.7	1.2	2.1	1.7	2.2	1.7	3.3					
IANIGLA-PV 437											3.6	2.3	3.5	2.2	5.0	1.9
IANIGLA-PV 441					1.6	1.1	1.7	1.6	2.0	1.7	2.8	2.1				
IANIGLA-PV 443									2.3	1.5	2.8	1.8	2.7	1.8		
IANIGLA-PV 445									2.8	1.9	3.3	2.3	3.8	2.5	4.8	2.3
IANIGLA-PV 448					2.3	1.2	2.2	1.7	2.5	1.8	3.3	2.2	2.8	2.3		
IANIGLA-PV 451					2.2	1.2	2.5	1.8	3.2	1.8	3.8	2.5	4.0	2.5	5.1	2.1
IANIGLA-PV 452									2.4	—	3.4	—				
IANIGLA-PV 456											3.1	2.1	3.0	2.4	4.8	2.2
IANIGLA-PV 457							2.3	1.5	2.6	2.0	3.4	2.3	3.3	2.4		
IANIGLA-PV 459					2.4	1.4	2.5	2.3	3.6	2.6						
IANIGLA-PV 465													4.0	2.3	5.0	2.2
IANIGLA-PV 468													3.9	2.1	5.1	2.2
IANIGLA-PV 476											3.3	2.3	3.8	2.3	5.0	2.2
IANIGLA-PV 478									2.7	2.0	3.5	2.5				
IANIGLA-PV 479					1.5	1.3	2.3	1.9	3.0	2.2	3.3	2.1	3.7	2.5	5.0	2.2
IANIGLA-PV 480													3.0	1.8	3.1	1.3
IANIGLA-PV 482									2.6	1.7	3.1	2.1	3.3	2.1	5.0	1.9
IANIGLA-PV 483							1.7	1.7	2.4	2.0						
IANIGLA-PV 484											3.3	2.3	3.3	2.3	4.7	2.3
IANIGLA-PV 485											3.3	2.5	3.5	2.4	4.4	2.2
IANIGLA-PV 486					1.3	1.0	2.2	1.6	2.5	—	3.0	2.2	3.3	2.1	4.5	2.0
IANIGLA-PV 490	2.9	—	2.8	—	2.3	1.2	2.5	1.9	2.9	1.9	3.6	2.1	3.6	2.2	4.9	1.9
IANIGLA-PV 496					1.6	1.2	2.4	1.6	3.3	2.0	3.7	2.3	3.9	2.4	5.0	2.1
IANIGLA-PV 499									3.2	2.1	3.9	2.6	3.8	2.6		
IANIGLA-PV 503					1.5	1.0	1.9	1.4	—	1.8	3.5	2.0	—	—	—	1.9
IANIGLA-PV 504					2.0	1.4	—	1.9	3.3	2.0	3.8	2.3	3.7	2.2		
IANIGLA-PV 508					1.5	0.9	1.7	1.2	2.0	1.6						
IANIGLA-PV 510					1.6	1.0	2.2	1.4	2.1	1.6	2.9	1.9	2.9	2.0	4.2	1.9
IANIGLA-PV 549							2.3	1.7	2.4	2.0	3.1	2.3	3.4	2.3	4.7	2.0
IANIGLA-PV 554	2.1	0.9	1.6	0.8	1.5	0.9	1.8	1.3	2.0	1.6	2.9	1.8	3.1	2.1	4.0	1.9
IANIGLA-PV 555							2.0	1.7	2.5	2.1	3.4	2.5	3.8	2.6	5.2	2.5
IANIGLA-PV 557	3.5	—	1.4	1.1	—	—	2.1	1.7	3.0	2.0	3.7	2.3	4.0	2.5	5.3	2.4
IANIGLA-PV 559							2.5	1.7	—	—	3.6	2.3	3.6	2.3	4.8	2.1
IANIGLA-PV 560	2.9	0.9		2.0	1.2	2.1	1.8	2.4	2.0	3.2	2.3	2.0				
IANIGLA-PV 561											3.0	1.8	3.2	1.9	4.4	—
IANIGLA-PV 562	3.6	1.1	2.6	1.0	1.7	1.1	2.3	1.7	2.4	1.9	3.3	1.7	3.4	1.8	4.3	2.1
MACN-A 8502	3.4	1.0	1.5	0.9	1.9	1.0	2.1	1.6	2.5	2.1	3.2	2.1	3.7	2.2	4.8	1.6
MACN-A 2434	3.6	1.2	2.3	1.1	—	—	2.4	2.0	2.7	2.1	3.5	2.3	3.5	2.3	4.9	2.2
MACN-Pv 1673							2.4	1.7	2.8	2.0	—	—	3.7	2.5	4.9	2.0
<i>Paedotherium typicum</i>																
IANIGLA-PV 23	5.1	1.5	2.4	1.3	2.3	1.8	2.9	2.6	3.5	2.9	4.8	2.8	4.2	2.8	6.1	2.8
IANIGLA-PV 477									3.7	2.5	4.0	2.9				
MACN-A 10267-68					2.3	1.5	3.9	2.4	3.8	2.5	4.2	2.5	3.8	2.4	6.0	2.4
MLP 12-1782	4.1	1.3	3.2	1.3	—	—	3.9	2.2	3.9	2.4	4.1	2.8	4.3	2.6	5.9	2.5
MLP 12-1783									3.7	2.6	4.1	2.8	4.2	2.6	5.8	2.2
MLP 12-1788							4.3	2.6	—	—	4.0	2.9	4.2	(3.0)	6.3	2.6
MLP 91-IV-5-6 (<i>P. insigne</i>)	5.1	1.7	2.4	1.8	2.5	1.5	4.2	2.6	4.3	2.8	4.1	2.7	4.3	2.7	6.3	—
S. Sal. Scar. Paleo 2012-045									3.8	2.6	4.4	2.2	4.7	2.4	5.7	2.2
YPM-VPPU 015682																
(<i>Pachyrukhos moyani</i>)	4.9	2.1	—	—	2.3	1.6	3.9	3.0	4.0	3.0	3.4	3.0	4.9	3.1	6.0	2.7

—, missing data; approximate values in parentheses.

MACN-Pv 8516, MACN-Pv 8517, and MACN-Pv 8519, that display the diagnostic characteristics of the genus *Paedotherium*, such as a lingual sulcus in P3, molarized P4, and M3 longer than M2. Since Rovereto's (1914) mention of *Pachyrukhos* sp., similar to *P. typicum*, *Paedotherium* specimens have never been

definitively identified at the species level at the Huayquerías del Este locality. In comparison with the large sample of *Tremacyllus* specimens from Huayquerías, the new material identified as *Paedotherium* is really scarce. Therefore, morphological comparison with better-known species of *Paedotherium* (e.g., *Paedotherium*



minor, *P. typicum*, *P. borrelloii*, *P. bonaerense*), combined with the morphometric geometric results presented above, allows us to identify our material as *Paedotherium typicum* in the Huayquerías Formation and possibly in the Tunuyán Formation (see below).

Referred Material—Huayquerías Formation. Huayquería de la Horqueta sur: IANIGLA-PV 23, mandible with right i1, [right] p2–m3, left i1–2, and [left] p2–m3; IANIGLA-PV 106, dentary with right p4–m3; IANIGLA-PV 469, maxillary fragment with right P3–4. Beautiful Canyon: IANIGLA-PV 507, maxillary fragment with left M2–3; IANIGLA-PV 556, poorly preserved skull with right and left I1 and P2–M3. Loma alta norte: IANIGLA-PV 460, dentary with broken left p4–m2; IANIGLA-PV 477, dentary with right p4–m1. Unknown location. MACN-Pv 8516, maxillary fragment with left P3(broken)–M3; MACN-Pv 8517, palate with right P2–M1; MACN-Pv 8519, maxillary fragment with left P3–M1.

Diagnosis—Apomorphy of the taxon: bilobed p2. Differs from *P. borrelloii* and *P. bonaerense* in moderately developed antorbital process; posterior nasal border at the level of the lacrimal bone; moderate zygomatic width; very inflated tympanic bullae in relation to skull size; mastoid bullae strongly developed beyond condyles; high and narrow occipital; short mandibular symphysis; more imbricated premolars and relatively shorter premolar series; relatively more curved P2–M3 rows; P2 very similar to P3; well-differentiated distolingual groove in all premolars, but typically shallower in P4; less-developed large entepicondyle of humerus; and curved femur. Differing from *P. minor* by larger size; similar or more square outline of P2–3; slightly or clearly more molarized P3/p3–P4/p4; M3 distally wider and much longer than M2; and more triangular third lobe in m3. *Paedotherium typicum* differs from *P. kakai* and *P. dolichognathus* in having, respectively, labial cementum on lowers molars and a shorter palate.

Description and Comparisons

Skull and Upper Dentition—IANIGLA-PV 556, although dorsally broken, is the most complete specimen, preserving palate, anterior part of right zygoma, and broken right bulla tympanica (Fig. 8A). The palate has a maximum length of 49.4 mm, and its width varies little between P2s ($W = 14.5$ mm) and M3s ($W = 16.3$ mm). The P2–M3 rows are slightly convex in comparison with the much more curved rows in *Tremacyllus*. The ventral surface of the premaxillae is broken (excavated), preventing observation of some relict of postincisor foramen depressions. Their length is proportionally shorter than in *Tremacyllus*. The anterior part of the zygoma is dorsoventrally flat and wide (11.6 mm), occupying the length of M2–3. The tympanic bulla is very inflated and well extended on the basicranium, similarly to other *Paedotherium* specimens (e.g., *P. typicum*; MMP 1008-M), and larger than in *Tremacyllus*.

The I1 of IANIGLA-PV 556 is a long and narrow tooth, labially convex and lingually concave; its anterior edge is square, whereas the posterior edge is pointed and narrower (Fig. 8A; Table 1). The P2–3 are subtriangular in outline, labially convex, lingually undulating with a shallow sulcus that forms a recognizable small lobe at the distal corner; P4 also displays the distal sulcus and has a smoothly convex ectoloph. Premolar size increases markedly from P2 to P4 (Table 1). The P3 has a mesially well-extended parastyle that overlaps P2 (Fig. 8B); lingually, the parastyle is delimited by a constriction conferring a concave mesial face to the P2–3. In P2 and P4, the parastyle is less developed than in P3.

Molars are characterized by their rectangular outline and being wider than P4 (Table 1), with straighter mesial and labial

faces and absence of a lingual sulcus (Fig. 8A). A pointed and externally folded parastyle is a conspicuous feature of M1–3 (Fig. 8A, D); M1–2 have a folded metastyle and a smoothly developed central fold in the ectoloph. The M3 is the longest tooth of the molar series (Table 1) and has a wide distal face, differing from M1–2 and the condition observed in *Tremacyllus impressus*. Cement covers the lingual face and the lingual part of the mesial face of P2–M3 (Fig. 8A–C), as was described for *Tremacyllus*, *Paedotherium minor*, and *P. bonaerense*.

The specimens from Rovereto's collection, MACN-Pv 8517 (right P2–M1; Fig. 8B) and MACN-Pv 8519 (left P2–4; Fig. 8C), are characterized by having labially convex P2–4 with a distolingual groove (slightly reduced in P4) that forms a recognizable distal lobe; this latter feature matches the condition in IANIGLA-PV 556, although it is a bit larger (Table 1). A similar groove is observed in P2–4 of other specimens attributed to *Paedotherium typicum* (e.g., MLP 12–1782, MLP 91-IV-5-66), *P. minor* (e.g., MLP 29-IX-1-116, holotype), and some specimens of *P. borrelloii* (e.g., MLP 57-X-10-88, holotype), whereas in *P. bonaerense* (e.g., MACN-Pv 1184) the lingual sulcus is absent in both P3 and P4 (Cerdeño and Bond, 1998; Ercoli et al., 2017).

The moderately molarized condition of P4 in the specimens from Mendoza is more similar to *P. typicum* than to *P. minor* (with typically less molarized P4), and clearly different from *P. borrelloii* and *P. bonaerense*, which have a much more molarized P4 (Ercoli et al., 2017). In addition, the studied sample differs from *P. borrelloii* and *P. bonaerense* in having more imbricated premolars, a variable lingual margin in M2, a shape from convex (Fig. 8A) to flat (Fig. 8D), and a distally narrower M3. *Paedotherium typicum* typically presents a proportionally longer M3 (Table 1) than does *P. minor*. Additionally, the size and degree of widening of the anterior region of the palate of the specimens from Mendoza are more similar to *P. typicum* specimens from other localities (in which the distance between P2s is similar to the distance between M3s) than *P. minor*, albeit some degree of overlap in these features is observed for some representatives of these species. Compared to *P. dolichognathus* (holotype MLP 69-IV-6-1), *P. typicum* possesses a shorter palate.

Mandible and Lower Dentition—The symphysis is wider and longer than in *Tremacyllus*, very procumbent, and its posterior border is at the p3 or p4 level (IANIGLA-PV 23; Fig. 8E–H); there is a well-marked masseteric crest at the m1–2 level, near the inferior border of the ramus, as also occurs in other specimens assigned to *P. typicum* (e.g., MACN-Pv 16679). There is a foramen below the p2 and m1 talonids on the labial face of the horizontal ramus of the mandible (Fig. 8E).

The i1 (Fig. 8E–F) is a long and flattened tooth with a rectangular outline, labially convex and lingually concave; the i2 is shorter, approximately half the size of i1 (Table 2; Fig. 8F).

The p2 is labially bilobed, with the distal lobe being the widest and the mesial lobe anteriorly directed (Fig. 8E, G); in some specimens of *P. typicum* (e.g., MLP 12–1782), the p2 is proportionally more elongated than in IANIGLA-PV 23 (Table 2). The p3 is completely different from p2; it is distinguished by a square and labially convex trigonid and a triangular talonid, although the talonid of p3 is broken (Fig. 8G). The p4 differs from p3 mainly by its longer and wider talonid, which is wider than the trigonid and has a concave distal face. The talonid of p3 is as wide as the trigonid, whereas in p4 the talonid is wider than the trigonid, a feature that also characterizes the molars (see below).

The m1–2 are similar to each other; they have triangular trigonid and talonid and a convex lingual face, differing from p4, which has a squarer trigonid and a distally concave talonid. In

←FIGURE 8. Upper and lower dentition of *Paedotherium typicum* from Mendoza. **A**, IANIGLA-PV 556, poorly preserved skull with right and left I1, and P2–M3, in occlusal view; **B**, MACN-Pv 8517, maxillary fragment with right P2–M1; **C**, MACN-Pv 8517, maxillary fragment with left P2–4; **D**, IANIGLA-PV 507, maxillary fragment with left M2–3; **E–H**, IANIGLA-PV 23, mandible with right i1, [right and left] p2–m3, and left i1–2, in occlusal view (**E**), detail of incisors (**F**), detail of right p2–m2 series (**G**), and in lateral view (**H**). Scale bars equal 5 mm.

m1–2 of IANIGLA-PV 23 (Fig. 8E, G; Table 2), the lingual face ends in a small distal lobe. Like m1–2, m3 has triangular trigonid and talonid but differs from m1–2 by having a third, posterior lobe that is elongated and narrower than the talonid, and a more convex lingual face (Fig. 8E). A thick layer of cementum covers the labial face of p2–m3, and the enamel is absent mesiolabially and distolingually (Fig. 8E, G).

Paedotherium typicum (e.g., IANIGLA-PV 23) differs from *P. minor* (e.g., MLP 29-IX-2-102, MLP 55-IV-28-57) in the morphology of p2; in the latter species, the p2 is labially trilobed (giving a ‘W’-shape to the occlusal surface), with a well-developed mesial lobe, a labially convex mesial lobe, and a transversely oriented and wider distal lobe; in addition, the p3 is less molarized and the m3 has a more rounded third lobe, and typically smaller size (e.g., lower values for linear measures of the teeth; Fig. 4B).

Paedotherium typicum differs from *P. kakai* (S. Sal. Scar. Paleo. 2012-045; Reguero et al., 2015; Table 2) in having cementum around the labial face of the molars. Another difference

concerns the height of the horizontal ramus of the mandible, which markedly increases anteriorly in *P. typicum*; *P. kakai* has a relatively low horizontal ramus with a peculiar labial crest, which is ‘S’-shaped, extending from the middle of m2, and lacking cementum in the cheek teeth. With respect to *P. borrelloii*, *P. typicum* has a less molarized p3 with a shorter talonid, less undulating lingual face on lower cheek teeth, and a relatively short premolar series.

Phylogenetic Analysis

The cladistic analysis resulted in 12 most parsimonious trees (MPTs; length = 52; consistency index [CI] = 0.73; retention index [RI] = 0.59). The consensus topology of these MPTs shows four nodes (Fig. 9A). Node A separates the outgroup *Hegetotherium mirabile*, the only Hegetotheriinae representative, from the ingroup, which comprises the Pachyrukhinae subfamily (node B, Fig. 9A), with high support for the clade. However, within

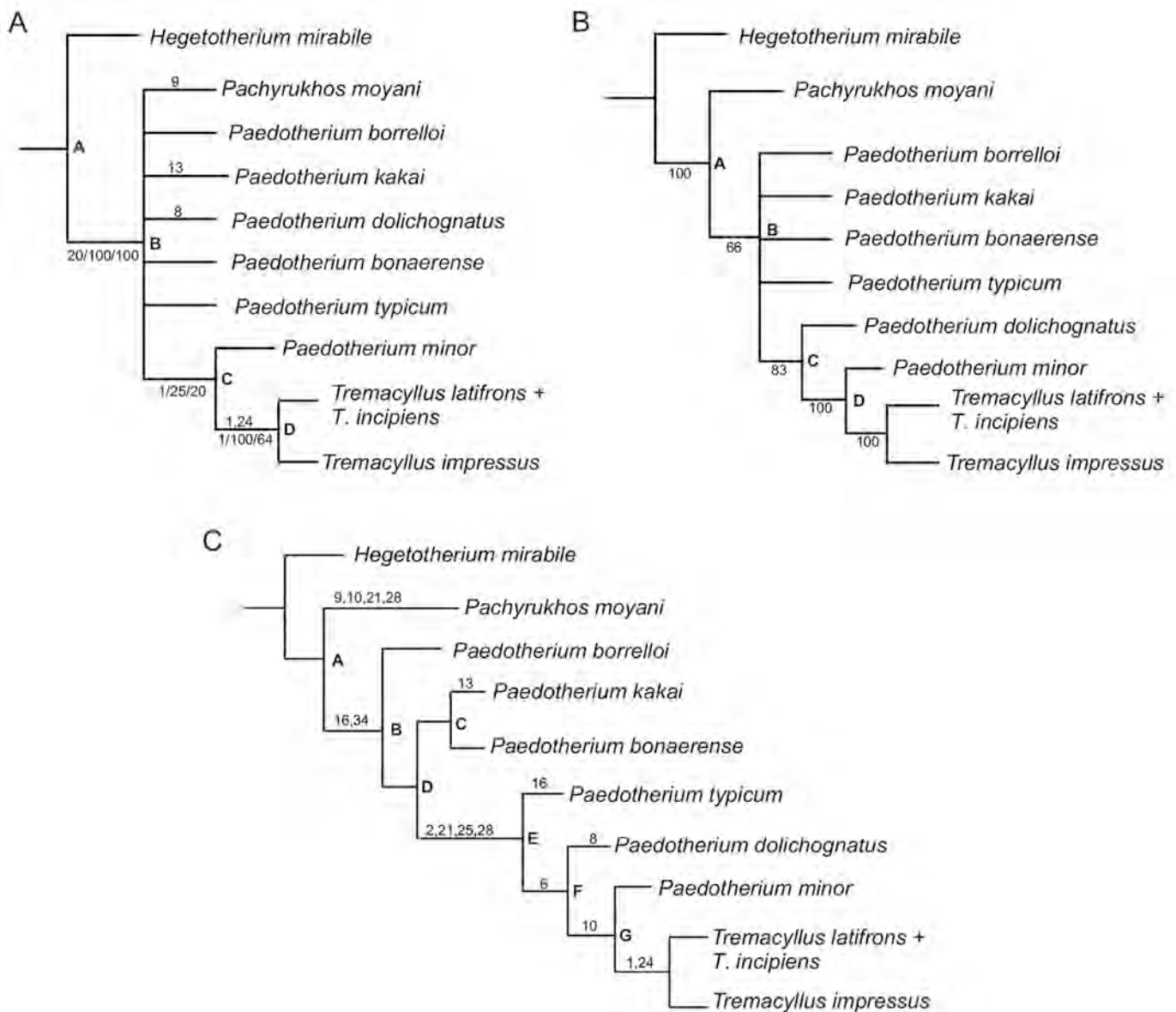


FIGURE 9. **A**, strict consensus topology of 12 most parsimonious trees (MPTs; length = 52; CI = 0.73; RI = 0.59) obtained in the phylogenetic analysis; **B**, the majority rule tree (from 12 trees, cut 50); **C**, one of the possible solutions among the 12 MPTs. Numbers above and below branches indicate apomorphies and Bremer and Jackknife indices, respectively.

node B, relationships are not well established because of a large polytomy: *Pachyrukhos moyani*, most of the species of *Paedotherium* (e.g., *P. moyani*, *P. borrelloii*, *P. kakai*), and node C. This polytomy is mainly due to the alternative positions taken by the poorly coded *P. borrelloii*, *P. kakai*, and *P. dolichognatus* among the 12 MPTs (see Supplementary Data 2). The most interesting result concerns node C, which groups *Paedotherium minor* plus *Tremacyllus* spp., a group recovered in the strict consensus (Fig. 9A), but no synapomorphy supports this assemblage (but see below); this group was also obtained by Ercoli et al. (2017: fig. 10), and is supported in their analysis by landmark character changes but no discrete characters. In turn, within node C, *Paedotherium minor* appears as the sister taxon of a clade comprising the species of *Tremacyllus* (node D, Fig. 9A). The genus *Tremacyllus* constitutes a well-supported monophyletic group (node D) with high Bremer and Jackknife indices and two synapomorphies: absence of lingual groove on upper premolars (character 1, state 0) and incisive foramina reaching premolar series (character 24, state 1).

Alternatively, the majority rule tree (from 12 trees, cut 50) resulted in a rather better-resolved topology (Fig. 9B) for the polytomy observed in the strict consensus (Fig. 9A). On the one hand, *Pachyrukhos moyani* is recovered as an early-diverging taxon from node A in 66% of the trees, as the sister taxon of node B, which groups the genera *Paedotherium* and *Tremacyllus*, agreeing with Ercoli et al. (2017:fig. 10). On the other hand, *Paedotherium dolichognatus* appears in 83% of the trees as the most diverging taxon from node C, which includes node D: *P. minor* plus *Tremacyllus* spp.

One of the possible solutions among the 12 MPTs (Fig. 9C) displays the relationships shown in Figure 9B, such as the position of *Pachyrukhos moyani* as the sister taxon of the clade *Paedotherium* spp. + *Tremacyllus* spp. (node B, Fig. 9C), which is supported by two synapomorphies: a labially trilobed p2 (character 16, state 1) and complete distal keel on metapodial (character 34, state 1). Within node B, *P. borrelloii* is the sister taxon of a more inclusive group (node D). This group gathers two lineages, one of them (node C) includes *P. kakai* and *P. bonaerense*, but no synapomorphies support the node, and the other (node E) is the clade (*P. typicum* (*P. dolichognatus* (*P. minor* (*Tremacyllus impressus*, *T. latifrons*/*T. incipiens*))), well-supported by four synapomorphies: very imbricated premolars (character 2, state 1), posterior nasal border at the lacrimal bone level (character 21, state 1), very inflated tympanic bulla (character 25, state 2), and mastoid bulla strongly developed beyond condyles (character 26, state 1). Regarding the three latter characters, it should be noted that they are unknown for *P. dolichognatus*, *P. kakai*, and *P. borrelloii*. In particular, regarding relationships within node E (Fig. 9C), it is interesting to note here the position of *P. dolichognatus*, a species based on a very fragmentary maxilla, and only 10 of 35 characters were coded for this taxon in our analysis (see Supplementary Data 2); however, its position as a sister taxon of node F, close to the *P. minor* + *Tremacyllus* spp. group, is sustained by one unambiguous synapomorphy: the non-molarized P4 (character 6, state 0).

In sum, our results confirm the paraphyletic condition of the genus *Paedotherium*, as was recently suggested (Ercoli et al., 2017; Seoane et al., 2017), and they are in concordance with the two main lineages proposed by Ercoli et al. (2017), which are represented by *P. bonaerense* and *P. typicum* (nodes C and E, Fig. 9C); however, relative to their analysis, we also included *P. kakai* and *P. dolichognatus*; the first appears closer to *P. bonaerense*, whereas the second groups closer to the *P. minor*–*Tremacyllus* clade. Our analysis thus proposes a different relationship at the basal node of this clade, considering *Paedotherium dolichognatus* closer to *P. minor* than *P. typicum*, and a more basal position for *P. borrelloii* in relation to *P. bonaerense* (both appear together in Ercoli et al., 2017).

Finally, in our analysis, the genus *Tremacyllus* is recovered as a monophyletic group, but not a single diagnostic feature differentiates the type species *T. impressus* from the *T. latifrons*/*T. incipiens* assemblage, agreeing with the evidence obtained by the morphogeometric analyses and traditional morphometric study presented herein. This should be taken into account when carrying out a revision of larger samples from other areas (e.g., Northwest Argentina), including the holotypes, in order to consider the number of species in the genus.

DISCUSSION

In the Huayquerías area sensu lato, Rovereto (1914) differentiated two horizons: the older ‘Araucanense’ and a transitional younger horizon between his Araucanense and the Hermosan. In the younger horizon, Rovereto erected *Tremacyllus subdiminutus* and mentioned the presence of *Pachyrukhos* sp. (= *Paedotherium*), referring to the latter as similar to *P. ‘typicum’* (= *P. typicum* and *P. bonaerense*) from Monte Hermoso (Buenos Aires Province); however, no description of this taxon has been provided since then. Based on new material recovered from Huayquerías del Este in Mendoza, we identified the two Pachyrukhinae genera in the area cited by Rovereto (1914); but unlike this author, we report *Tremacyllus* and *Paedotherium* records in both the Huayquerías and the Tunuyán formations.

In the case of *Tremacyllus*, *T. subdiminutus* was described by Rovereto (1914) only based on an incomplete palate (MACN-Pv 8494); however, the morphological comparison of the large sample of *Tremacyllus* from Mendoza analyzed here with better-known species of *Tremacyllus* (taking into account type material and referred specimens) described in other geographic areas (e.g., *Tremacyllus impressus*, *T. latifrons*, *T. incipiens*) and the morphometric geometric results presented here do not support a distinct species (*T. subdiminutus*) in Mendoza. Instead, we recognize *Tremacyllus impressus* in both the Huayquerías and Tunuyán formations, a proposition that involves the name *T. subdiminutus* becoming a junior synonym of *T. impressus*. The abundant new material from Mendoza allows us to describe new characters for both the upper and lower dentitions, as well as for some bones of the postcranium attributed to this species, expanding both the generic and specific diagnoses.

Following this reasoning, and analyzing the morphological variation of the large sample, *Tremacyllus impressus* is characterized by wide variability in some craniomandibular features (e.g., caudal projection of postforamen depressions), most of them represented by several polymorphisms (Supplementary Data 1–2), and many cheek tooth characters, mainly related to different degrees of widening and imbrication of the contour of the occlusal surfaces. The cause of this variation falls outside the scope of this contribution, but different ontogenetic stages, degrees of tooth wear, and stages of preservation could be involved in this continuum and the wide range of variation observed in some traits. This wide range of forms could explain the overestimation of the number of species of *Tremacyllus* in the past (see below).

Tremacyllus impressus was originally described from the Monte Hermoso Formation (Buenos Aires Province; Ameghino, 1888), early Pliocene (Tomassini et al., 2013); we here recognize its presence also in the Huayquerías and Tunuyán formations of Mendoza Province, which not only implies a new area in the distribution of *T. impressus* but also confirms the extension of its biochron back to the late Miocene (see also Cerdeño and Bond, 1998; Deschamps, 2005). On the other hand, no morphological differences were established between specimens from the Huayquerías Formation with respect to those coming from the overlying Tunuyán Formation.

Regarding other species of *Tremacyllus*, Rovereto (1914) described *T. incipiens* and *T. latifrons* from Catamarca Province. The author based both species on articulated skulls (holotypes

MACN-Pv 8163 and MACN-Pv 8157, respectively), which do not allow for establishing accurate dental comparisons, and no new material has been described for either taxon since Rovereto's publication. Nevertheless, Cerdeño and Bond (1998) postulated that *T. latifrons* is a synonym of *T. incipiens*, the latter being considered the valid species and the only species subsequently mentioned for Catamarca (e.g., Armella et al., 2015). In fact, the two skulls (MACN-Pv 8157 and MACN-Pv 8163) are externally so similar that they are not unlikely to represent the same species, as Cerdeño and Bond (1998) suggested. The synonymy proposed by Cerdeño and Bond (1998) was not justified by the authors. This situation highlights the need to carry out a review of both species (with more material at hand) and reevaluate the proposed synonymy. Here, based on the specimens attributed to *T. latifrons* (e.g., MACN-Pv 8169, FMNH P 14377, FMNH P 14399; see Appendices 1–2), we present comparisons between this species and *T. impressus* from Mendoza, but we cannot establish direct comparisons between these species and *T. incipiens* (articulated holotype). In fact, our geometric morphometric analyses indicate segregation between southern representatives of the genus (recognized as *T. impressus*) and the northern ones (most of them traditionally considered as *T. latifrons*, but including other specimens whose identity has not been adequately tested). The most interesting aspect of this analysis is that this latitudinal segregation disappears when we consider the specimens from Mendoza here identified as *T. impressus*, which broadly overlaps with both the southern and northern samples. This pattern could be an artifact of other factors already mentioned, such as morphological biases caused by ontogeny, wear, and/or preservation, in addition to the relatively poorly represented *Tremacyllus* samples from other areas in our analysis. It agrees with the phylogenetic analysis, where the genus *Tremacyllus* resulted in a well-supported monophyletic group (Fig. 9) with two synapomorphies (absence of lingual groove on upper premolars and incisive foramina reaching premolar series), but not a single diagnostic feature allows us to differentiate *T. impressus* from *T. latifrons* or *T. incipiens*. More and better-identified specimens are necessary to reinforce the hypothesis given the wide range of within-taxon variation.

In the case of *Paedotherium*, we certainly identify *P. typicum* in the Huayquerías Formation, mainly based on IANIGLA-PV 556 and IANIGLA-PV 23; on the other hand, the scarce and fragmentary nature of the remains from the Tunuyán Formation do not allow us to identify at level species between *P. typicum* and *P. minor*, two species that share many features. For instance, specimen IANIGLA-PV 514 (incomplete lower tooth series) from the Tunuyán Formation has a p3 that is closer to that of *P. minor* than that of *P. typicum*, although the size of the series fits with that expected for *P. typicum*. Additionally, the shape of m3 and IANIGLA-PV 447 and the M2–3 proportion of IANIGLA-PV 569 seems more similar to that observed in *P. typicum* than *P. minor*. More complete remains are necessary to confirm the presence of one or both species of *Paedotherium* in the Tunuyán Formation.

Based on the new material collected in the last five years, *Tremacyllus* is the most abundant notoungulate in the faunal association of the Huayquerías del Este area, with 92% of the record of hegetotheriids versus 8% for *Paedotherium* in the Huayquerías Formation, a dominance also pointed out by Zetti (1972a). In terms of the number of specimens, the record of *Tremacyllus* in the Huayquerías Formation (late Miocene) is significantly larger than that from the Tunuyán Formation (early Pliocene); in turn, the record of *Paedotherium* remains practically unchanged and of low frequency between the two formations in comparison with *Tremacyllus*, although a point to consider is that the Tunuyán Formation has been under-sampled with respect to the overlying Huayquerías Formation.

The high frequency of *Tremacyllus* specimens in the Huayquerías Formation assemblage is comparable to that of the

Andalhuálá Formation (Catamarca Province), which indicates that this taxon was an important component in the late Miocene communities of both western regions of Argentina, although *Tremacyllus* has not yet been recorded in the Palo Pintado Formation (Salta Province), where a single specimen of *Paedotherium* was described (Reguero et al., 2015).

This situation clearly contrasts with the inverse relation in the Pampean region, where *Paedotherium* is more abundant than *Tremacyllus*, in both sediments referred to the Huayquerian and to the Montehermosan (Zetti, 1972a; Cerdeño and Bond, 1998; Tomassini et al., 2017). It should be noted, however, that the eastern faunas are relatively younger than the western faunas, which could also explain this difference in the abundance of *Paedotherium* and *Tremacyllus*.

The presence of *Paedotherium typicum* in the Huayquerías Formation in the Huayquerías del Este area (Mendoza), and possibly in the Tunuyán Formation as well, implies not only a new geographic area in its distribution but also the oldest record for this species (i.e., late Miocene). The species was previously described only from the Pliocene of Buenos Aires and San Luis provinces (Ameghino, 1887a; Cerdeño and Bond, 1998; Prado et al., 1998). This conclusion has important implications for biogeography and evolution of the group. On the one hand, *Paedotherium typicum* should not be considered as an index taxon of post-Miocene faunas, because it is recorded in older rocks than previously documented. On the other hand, the presence of *P. typicum* during the late Miocene supports a recent hypothesis (Ercoli et al., 2017) proposing that this species is more closely related to the ancestral form, maintaining morphologically less modified cheek teeth, than to *P. minor* and *Tremacyllus* spp. This hypothesis, in turn, is linked to the proposal that the latter two taxa form the sister clade of *Paedotherium typicum* (Ercoli et al., 2017, and other contributions), an idea that is reinforced here by our phylogenetic analysis, results of which yielded *P. typicum* as the early-diverging taxon from a more inclusive clade (*P. dolichognatus* (*P. minor* (*Tremacyllus impressus*, *T. latifrons*/*T. incipiens*))).

CONCLUSIONS

Based on the new material of Pachyrukhinae from the Huayquerías del Este area (Mendoza, Argentina) presented here, we confirm the presence of *Tremacyllus* and *Paedotherium* in both the Huayquerías and Tunuyán formations.

The geometric morphometric methods applied on upper and lower dentition reveal that the specimens of *Tremacyllus* from Mendoza display a wide and continuous morphological variation that encompasses the morphological differences between species previously considered valid. Based on that and comparisons with well-known samples of *Tremacyllus*, we recognize the presence of *T. impressus*, proposing *T. subdiminutus* as a junior synonym. Regarding *Paedotherium*, the geometric morphometric analyses were not conclusive in separating *P. minor* from *P. typicum*, but the overall analysis of all information allows us to assign the sample from Mendoza to *P. typicum*, which shows a particular combination of features differing from other species of *Paedotherium* (e.g., moderately developed antorbital process, very inflated tympanic bullae size in relation to skull, mastoid bullae strongly developed beyond condyles, short mandibular symphysis, more imbricated premolars and relatively shorter premolar series, bilobed p2, relatively more curved P2–M3 rows, P2 very similar to P3, well-differentiated distolingual groove in all premolars, less-developed large entepicondyle of the humerus, and curved femur).

The new material attributed to *T. impressus* and *P. typicum* allows us to expand both the generic and the specific diagnosis; in the case of *T. impressus*, we provide new data on

postcranial bones, humerus, astragalus, calcaneum, navicular, and metatarsal.

Tremacyllus impressus and *Paedotherium typicum* coexist in the Huayquerías Formation; *T. impressus* is also present in the Tunuyán Formation, whereas the specimens recognized as *Paedotherium* in this unit are too fragmentary to identify at the species level.


The presence of *Tremacyllus impressus* and *Paedotherium typicum* in the late Miocene of Mendoza implies a geographic extension to the center-west Argentina of both taxa and the oldest record in the case of *P. typicum*.

Finally, based on morphological characters of the skull and postcranium, we performed a cladistic analysis including for the first time all the species presently recognized in *Paedotherium* and *Tremacyllus*. According to our results, the relationships in the genus *Paedotherium* are not well established, appearing as a paraphyletic assemblage in concordance with previous hypotheses, although a well-supported clade *P. minor* + *Tremacyllus* spp. was obtained. *Tremacyllus* formed a monophyletic group supported by two synapomorphies (absence of lingual groove on upper premolars and incisive foramina reaching premolar series); however, in this genus, no diagnostic features differentiate *T. impressus* from *T. latifrons* or *T. incipiens*, although more and better-identified specimens from northwestern Argentina are necessary to clarify the existence of only one or more species in the genus.

ACKNOWLEDGMENTS

We thank editors of the Journal, and K. Moreno and an anonymous reviewer for improving this manuscript. P. Ortiz and D. García-López (CML), W. Simpson and A. Stroup (FMNH), A. Rivero and N. Solís (IDGYM), S. Alvarez and A. Kramarz (MACN), M. Reguero (MLP), and M. Taglioretti, F. Scaglia, V. Sarasa, and A. Dondas (MMP) granted access to osteological materials under their care. A. Forasiepi (IANIGLA) and F. Prevosti (CRILAR) offered us the Pachyrukhinae sample from the Huayquerías. A. Álvarez (IDGYM, INECO), F. Gianechini (UNSL), L. Fiorelli (CRILAR), G. Cassini (MACN), and L. Cruz (MACN) provided photographic material. R. Bottero (IANIGLA) designed the map (Figure 1) and helped with figures. M.D.E. thanks IOM for facilitating a trip to U.S.A. to visit the FMNH collections. The research was financed by 'Consejo Nacional de Investigaciones Científicas y Técnicas' (CONICET, Argentina), and the field work was partially supported by 'Agencia Nacional de Promoción Científica y Técnica' (ANP-CyT, Argentina), project PICT 2015–966 (to F. Prevosti, CRILAR).

ORCID

Marcos D. Ercoli  <http://orcid.org/0000-0003-2695-2723>

LITERATURE CITED

- Ameghino, F. 1885. Nuevos restos de mamíferos fósiles oligocenos, recogidos por el profesor Pedro Scalabrini y pertenecientes al Museo Provincial de la Ciudad del Paraná. Boletín de la Academia Nacional de Ciencias en Córdoba 8:5–207.
- Ameghino, F. 1887a. Apuntes preliminares sobre algunos mamíferos estinguidos del yacimiento de Monte Hermoso existentes en el Museo La Plata. Boletín del Museo La Plata 1:1–20.
- Ameghino, F. 1887b. Observaciones generales sobre el orden de mamíferos estinguidos Sud-americanos llamados toxodontes (Toxodontia) y sinopsis de los géneros y especies hasta ahora conocidos. Anales del Museo de La Plata, (Entrega especial, 1936:1–66.
- Ameghino, F. 1888. Lista de las especies de mamíferos fósiles del Mioceno superior de Monte-Hermoso hasta ahora conocidas; in A. J. Torcelli (ed.), Obras Completas y Correspondencia Científica de Florentino Ameghino, Volumen 5. La Plata Taller de Impresiones Oficiales 1913-36, pp. 481–496.
- Ameghino, F. 1889. Contribución al conocimiento de los mamíferos fósiles de la República Argentina. Actas de la Academia Nacional de Ciencias de Córdoba 6:1–1027.
- Ameghino, F. 1891. Mamíferos y aves fósiles argentinas. Especies nuevas, adiciones y correcciones. Revista Argentina de Historia Natural 1:240–259.
- Ameghino, F. 1894. Enumération synoptique des espèces de mammifères fossiles des formations éocènes de Patagonie. Boletín de la Academia Nacional de Ciencias de Córdoba 13:259–445.
- Ameghino, F. 1908. Las formaciones sedimentarias de la región litoral de Mar del Plata y Chapalmalán. Anales del Museo Nacional de Buenos Aires 3:343–428.
- Armella, M. A., D. A. García López, and G. I. Esteban. 2015. Nuevo registro y revisión del género *Tremacyllus* (Pachyrukhinae, Hegetotheriidae, Notoungulata) del Mioceno tardío de la Provincia de Catamarca. XXIX Jornadas Argentinas de Paleontología de Vertebrados. Ameghiniana 52:R6.
- Bonini, R. A. 2014. Bioestratigrafía y diversidad de los mamíferos del Neógeno de San Fernando y Puerta de Corral Quemado (Catamarca, Argentina). Ph.D. dissertation, Universidad Nacional de La Plata, La Plata, Argentina, 366 pp.
- Bonini, R. A., A. M. Forasiepi, F. J. Prevosti, A. C. Garrido, D. L. Barbeau, G. F. Turazzini, S. Echarri, F. Pujos, R. Macphee, D. Verzi, B. Vera, E. Cerdeño, M. E. Pérez, L. L. Rasia, G. Esteban, and M. S. de la Fuente. 2016. Avances en paleontología, estratigrafía y edad de la Formación Huayquerías (Mioceno tardío, Mendoza). XXX Jornadas Argentinas de Paleontología de Vertebrados. Ameghiniana 53: R50.
- Brandoni, D., G. I. Schmidt, A. M. Candela, J. I. Noriega, E. Brunetto, and L. E. Fiorelli. 2012. Mammals from the Salicas Formation (late Miocene), La Rioja Province, northwestern Argentina: paleobiogeography, age, and paleoenvironment. Ameghiniana 49:375–387.
- Burmeister, C. V. 1888. Relación de un viaje a la gobernación del Chubut. Anales del Museo Nacional de Buenos Aires 3:175–252.
- Cabrera, A. 1937. Notas sobre el suborden "Tyotheria". Notas del Museo de La Plata 2:17–43.
- Cerdeño, E., and M. Bond. 1998. Taxonomic revision and phylogeny of *Paedotherium* and *Tremacyllus* (Pachyrukhinae, Hegetotheriidae, Notoungulata) from the Late Miocene to the Pleistocene of Argentina. Journal of Vertebrate Paleontology 18:799–811.
- Cerdeño, E., C. I. Montalvo, and R. Sostillo. 2017. Deciduous dentition and eruption pattern in late Miocene Pachyrukhinae (Hegetotheriidae, Notoungulata) from La Pampa Province, Argentina. Historical Biology 29:359–375.
- Cifelli, R. L. 1983. Eutherian tarsals from the late Paleocene of Brazil. American Museum Novitates 2761:1–31.
- Contreras, V. H., and J. A. Baraldo. 2011. Calibration of the Chasicuan-Huayquerian stages boundary (Neogene), San Juan, western Argentina; p. 111–121 in J. A. Salfity and R. A. Marquillas (eds), Cenozoic Geology of the Central Andes of Argentina. SCS Publisher, Salta, Argentina.
- Croft, D. A., and F. Anaya. 2006. A new middle Miocene hegetotheriid (Notoungulata: Tyotheria) and a phylogeny of the Hegetotheriidae. Journal of Vertebrate Paleontology 26:387–399.
- De Carles, E. 1911. Ensayo geológico descriptivo de las Guayquerías del Sur de Mendoza (Departamento de San Carlos). Anales del Museo Nacional de Historia Natural 22:77–95.
- Deschamps, C. M. 2005. Late Cenozoic mammal bio-chronostratigraphy in southwestern Buenos Aires Province, Argentina. Ameghiniana 42:733–750.
- Dessanti, R. N. 1946. Hallazgo de depósitos glaciares en las Huayquerías de San Carlos (Mendoza). Revista de la Sociedad Geológica Argentina 1:270–284.
- Echarri, S., A. M. Forasiepi, A. C. Garrido, F. J. Prevosti, G. F. Turazzini, and B. Vera. 2013. Las Huayquerías de Mendoza. Nuevos trabajos de campo y resultados preliminares. II Simposio del Mioceno-Plioceno del Centro y Norte de Argentina. Ameghiniana 50:R10.
- Elissamburu, A. 2004. Análisis morfométrico y morfofuncional del esqueleto apendicular de *Paedotherium* (Mammalia, Notoungulata). Ameghiniana 41:363–380.
- Elissamburu, A., and S. F. Vizcaino 2005. Diferenciación morfométrica del húmero y fémur de las especies de *Paedotherium* (Mammalia, Notoungulata) del Plioceno y Pleistoceno temprano. Ameghiniana 42:159–166.

- Ercoli, M. D., A. M. Candela, L. L. Rasia, and M. A. Ramírez. 2017. Dental shape variation of Neogene Pachyrukhinae (Mammalia, Notoungulata, Hegetotheriidae): systematics and evolutionary implications for the late Miocene *Paedotherium* species. *Journal of Systematic Palaeontology*. doi: 10.1080/14772019.2017.1366956
- Folguera, A., and M. Zárate. 2009. La sedimentación neógena continental en el sector extrandino de Argentina central. *Revista de la Asociación Geológica Argentina* 64:692–712.
- Folguera, A., and M. Zárate. 2011. Neogene sedimentation in the Argentine foreland between 34°30'S and 41°S and its relation to the Andes evolution; pp. 123–134 in J. A. Salfity and R. A. Marquillas (eds.), *Cenozoic Geology of the Central Andes of Argentina*. SCS Publisher, Salta, Argentina.
- Forasiepi, A. M., R. MacPhee, S. Hernández del Pino, G. I. Schmidt, E. Amson, and C. Grohé. 2016. Exceptional skull of *Huayqueriana* (Mammalia, Litopterna, Macrauchenidae) from the late Miocene of Argentina: anatomy, systematics, and paleobiological implications. *Bulletin of the American Museum of Natural History* 404:1–76.
- Forasiepi, A. M., F. J. Prevosti, A. C. Garrido, B. Vera, G. F. Turazzini, S. Echarri, R. Bonini, F. Pujos, R. MacPhee, D. Verzi, L. L. Rasia, G. I. Schmidt, G. Esteban, and V. Krapovickas. 2015. Avances en el conocimiento de la fauna de la Formación Huayquerías (Mioceno Tardío, Mendoza). III Simposio del Mioceno-Plioceno del Centro y Norte de Argentina. *Ameghiniana* 53:R12.
- Garrido, A. C., R. Bonini, and D. L. Barbeau. 2017. Paleoambiente, edad y vertebrados de la Formación Huayquerías (Mioceno tardío), Provincia de Mendoza, República Argentina. XX Congreso Geológico Argentino. IV Simposio del Mioceno-Plioceno del Centro y Norte de Argentina. *Actas Simposio* 1:50–55.
- Garrido, A. C., G. F. Turazzini, M. Bond, G. Aguirrezabala, and A. M. Forasiepi. 2014. Estratigrafía, vertebrados fósiles y evolución tectosedimentaria de los depósitos neógenos del Bloque de San Rafael (Mioceno-Plioceno), Mendoza, Argentina. *Acta Geológica Lilloana* 26:133–164.
- Goloboff, P., J. S. Farris, and K. Nixon. 2008. TNT, a free program for phylogenetic analysis. *Cladistics* 24:774–786.
- Goloboff, P. A., J. S. Farris, M. Källersjö, B. Oxelman, M. J. Ramírez, and C. A. Szumik. 2003. Improvements to resampling measures of group support. *Cladistics* 19:324–332.
- Groeber, P. 1939. Mapa geológico de Mendoza. *Physis, Revista de la Sociedad Argentina de Ciencias Naturales* 14:171–230.
- Kraglievich, L. 1926. Sobre el conducto humeral en las vizcachas y paquirucos chapadmalenses con descripción del *Paedotherium imperforatum*. *Anales del Museo de Historia Natural Bernardino Rivadavia* 34:45–88.
- Kraglievich, L. 1934. La antigüedad pliocena de las faunas de Monte Hermoso y Chapadmalal, deducidas de su comparación con las que le precedieron y sucedieron. *El Siglo Ilustrado*, Montevideo, 136 pp.
- Linares, O. J. 1981. Tres nuevos carnívoros prociénidos fósiles del Mioceno de Norte y Sudamérica. *Ameghiniana* 18:113–121.
- Marshall, L. G., R. E. Drake, and G. H. Curtis. 1986. ^{40}K – ^{40}Ar calibration of Late Miocene-Pliocene mammal-bearing Huayquerías and Tunuyán formations, Mendoza province, Argentina. *Journal of Paleontology* 60:448–457.
- Montalvo, C. I., and S. Casadío. 1988. Presencia del género *Palaeoctodon* (Rodentia, Octodontidae) en el Huayqueriense (Mioceno tardío) de la Provincia de La Pampa. *Ameghiniana* 25:111–114.
- Montalvo, C. I., G. Visconti, L. Pugener, and M. C. Cardonatto. 1995. Mamíferos de Edad Huayqueriense (Mioceno tardío), Laguna Chillhué, provincia de La Pampa. IV Jornadas Geológicas y Geofísicas Bonaerenses, Junín, Buenos Aires, 15–17 November 1995. *Actas, Volumen* 1:73–79.
- Nasif, N., and S. M. Georgieff. 2014. Cronobioestratigrafía del Mioceno tardío—Plioceno temprano, Puerta de Corral Quemado y Villavil, provincia de Catamarca, Argentina. *Acta Geológica Lilloana* 26:165–192.
- Prado, J. L., J. Chiesa, G. Tognelli, E. Cerdeño, and E. Strasser. 1998. Los mamíferos de la Formación Río Quinto (Plioceno), Provincia de San Luis (Argentina). Aspectos bioestratigráficos, zoogeográficos y paleoambientales. *Estudios Geológicos* 54:153–160.
- Reguero, M. A., A. M. Candela, C. I. Galli, R. Bonini, and D. Voglino. 2015. A new Hysodont Notoungulate (Hegetotheriidae, Pachyrukhinae) from the late Miocene of the Eastern Cordillera, Salta province, Northwest of Argentina. *Andean Geology* 42:56–70.
- Riggs, E. S., and B. Patterson. 1939. Stratigraphy of the Late-Miocene and Pliocene deposits of the Province of Catamarca (Argentina) with notes on the faunas. *Physis* 14:143–162.
- Roth, S. 1903. Los ungulados sudamericanos. *Anales del Museo La Plata, Paleontología Argentina* 5:1–36.
- Rovereto, C. 1914. Los estratos araucanos y sus fósiles. *Anales del Museo Nacional de Historia Natural* 25:1–247.
- Rusconi, C. 1939. Lista de mamíferos miocénicos de las Huayquerías de Mendoza. *Physis* 14:461–654.
- Seoane, F. D., S. Roig Juárez, and E. Cerdeño. 2017. Phylogeny and paleobiogeography of Hegetotheriidae (Mammalia, Notoungulata). *Journal of Vertebrate Paleontology*. doi: 10.1080/02724634.2017.1278547.
- Simpson, G. G. 1940. Review of the mammal-bearing Tertiary of South America. *Proceedings of the American Philosophical Society* 83:649–709.
- Sinclair, W. J. 1909. Typotheria of the Santa Cruz beds. Reports of the Princeton University Expedition to Patagonia, 1896–1899 6:1–110.
- Sostillo, R., C. I. Montalvo, and E. Cerdeño. 2012. Los Pachyrukhinae (Hegetotheriidae, Notoungulata) de Salinas Grandes de Hidalgo, Formación Cerro Azul, Mioceno tardío, La Pampa. *Ameghiniana* 49:R57.
- Tauber, A. A. 2005. Mamíferos fósiles y edad de la Formación Salicas (Mioceno tardío) de la sierra de Velasco, La Rioja, Argentina. *Ameghiniana* 42:443–460.
- Tauber, A. A., J. M. Krapovickas, H. Marengo, and A. Haro. 2014. Paleontología del Cenozoico. XIX Congreso Geológico Argentino Geología, Córdoba, 2–6 June 2014. *Relatorio*:591–621.
- Tomassini, R. L., M. C. Garrone, and C. I. Montalvo. 2017. New light on the endemic South American pachyrukhine *Paedotherium* Burmeister, 1888 (Notoungulata, Hegetotheriidae): taphonomic and paleohistological analysis. *Journal of South American Earth Sciences* 73:33–41.
- Tomassini, R. L., C. I. Montalvo, C. M. Deschamps, and T. Manera. 2013. Biostratigraphy and biochronology of the Monte Hermoso Formation (early Pliocene) at its type locality, Buenos Aires Province, Argentina. *Journal of South American Earth Sciences* 48:31–42.
- Vera, B. 2016. Phylogenetic revision of the South American notopithecines (Mammalia, Notoungulata). *Journal of Systematic Palaeontology* 14:461–480.
- Vera, B., and E. Cerdeño. 2014. New insights on *Antepithecus brachystephanus* Ameghino, 1901 and dental eruption sequence in 'notopithecines' (Mammalia, Notoungulata) from the Eocene of Patagonia, Argentina. *Geobios* 47:165–181.
- Vera, B., and M. D. Ercoli. 2017. Estudio sistemático y morfo-geométrico de los Pachyrukhinae (Hegetotheriidae) de las Huayquerías de San Carlos, Bahía Blanca, Argentina, 14–17 November 2017. *Abstracts*:175.
- Verzi, D. H., C. I. Montalvo, and C. M. Deschamps. 2008. Biochronology and biostratigraphy of the Upper Miocene of central Argentina: evidence from rodents and taphonomy. *Geobios* 41:145–155.
- Verzi, D. H., C. I. Montalvo, and M. G. Vucetich. 1999. Afinidades y significado evolutivo de *Neophanomys biplicatus* (Rodentia Octodontidae) del Mioceno tardío-Plioceno temprano de Argentina. *Ameghiniana* 36:83–90.
- Yrigoyen, M. R. 1993. Los depósitos sinorogénicos terciarios. Geología y recursos naturales de Mendoza. In V. A. Ramos (ed.), XII Congreso Geológico Argentino y II Congreso de Explotación de Hidrocarburos, Mendoza, Argentina, 10–15 October 1993. *Relatorio*: 123–148.
- Yrigoyen, M. R. 1994. Revisión estratigráfica del Neógeno de las Huayquerías de Mendoza septentrional, Argentina. *Ameghiniana* 31:125–138.
- Zetti, J. 1972a. Los mamíferos fósiles de edad huayqueriense (Plioceno medio) de la región pampeana. Ph.D. dissertation, Universidad de La Plata, La Plata, Argentina, 100 pp.
- Zetti, J. 1972b. Observaciones sobre los Pachyrukhinae (Notoungulata) del Plioceno argentino. *Publicaciones del Museo Municipal de Ciencias Naturales de Mar del Plata* 2:41–52.

Submitted December 21, 2017; revisions received March 8, 2018; accepted March 10, 2018.

Handling editor: Marcelo Sanchez-Villagra.

APPENDIX 1. List of specimens included in the upper cheek tooth analyses.

P2–M3 Analysis

Pachyrukhos moyani: AMNH FM 15743, FMNH P 13049, FMNH P 13053, FMNH P 12994, MACN-A 279/296

Paedotherium bonaerense: FMNH P 14330, IDGYM sn, MACN-A 10269, MACN-Pv 10515, MACN-Pv 18098/18100, MACN-Pv 10513/10514, MACN-A 1251/1252, MACN-Pv 1081, MACN-Pv 7214, MACN-Pv 7253, MACN-A 10267/10268, MACN-Pv 1184, MACN-Pv 7732, MLP 99-X-2-1, PVL 503, PVL 2272, PVL 2377

Paedotherium borrelloii: MLP 57-X-10-21, MLP 57-X-10-88

Paedotherium minor: MLP 29-IX-2-157, MLP 29-IX-1-152, MLP 26-IV-10-19, MLP 29-IX-1-116, MLP 55-IV-28-30, MLP 29-IX-2-120, MLP 29-IX-2-5, MLP 76-VI-12-91

Paedotherium typicum: MACN-Pv 6436, MACN-Pv 11003, MACN-Pv 16752, MACN-Pv 17333, MACN-Pv 10027, MACN-A 5755, MLP 91-IV-5-63, MLP 91-IV-5-69, MHIN UNSL GEO V 531, MLP 52-IX-28-14, MUFyCA 374, PVL 3386

Paedotherium specimen from Mendoza: IANIGLA-PV 556

Tremacyllus latifrons: FMNH P 14377, FMNH P 14399, FMNH P 14456

Tremacyllus cf. latifrons: FMNH P 14465, FMNH P 15254

Tremacyllus impressus: MACN-Pv 2434, MACN-Pv 2913, MACN-A 1377

Tremacyllus cf. impressus, MACN-Pv 16916

Specimens of *Tremacyllus* from Mendoza: IANIGLA-PV 553, IANIGLA-PV 555, IANIGLA-PV 565/566, MACN-Pv 8497, MACN-Pv 8495, MACN-Pv 8494

P3–M2 Analysis

Pachyrukhos moyani: AMNH FM 15743, FMNH P 13049, FMNH P 13053, FMNH P 12994, MACN-A 279/296, MACN-A 319/321

Paedotherium bonaerense: FMNH P 14330, IDGYM sn, MACN-A 10269, MACN-Pv 10515, MACN-Pv 18098/18100, MACN-Pv 10513/10514, MACN-A 1251/1252, MACN-Pv 1081, MACN-Pv 7214, MACN-Pv 7253, MACN-A 10267/10268, MACN-Pv 1184, MACN-Pv 7732, MACN-A 1670, MLP 12-1785, MLP 32-IX-27-39, MLP 99-X-2-1, MUFyCA 374, PVL 2272, PVL 2377, PVL 503, PVL 500/502

Paedotherium borrelloii: MLP 57-X-10-21, MLP 57-X-10-88, MLP 57-X-10-70/78 (I), MLP 57-X-10-70/78 (II), MLP 57-X-10-146, MLP 65-VII-29-52

Paedotherium minor: MLP 29-IX-2-157, MLP 29-IX-1-152, MLP 26-IV-10-19, MLP 29-IX-1-116, MLP 55-IV-28-30, MLP 29-IX-2-120, MLP 29-IX-2-5, MLP 76-VI-12-91, MLP 29-IX-2-119/121

Paedotherium typicum: MHIN UNSL GEO V 531, MACN-Pv 6436, MACN-A 5755, MACN-Pv 11003, MACN-Pv 16752, MACN-Pv 17333, MACN-Pv 10027, MLP 91-IV-5-69, MLP 52-IX-28-14, MLP 12-1782, MLP 91-IV-5-63, MLP 91-IV-5-62, MLP 91-IV-5-58, PVL 3386

Paedotherium specimen from Mendoza: IANIGLA-PV 556

Tremacyllus latifrons: FMNH P 14377, FMNH P 14399, FMNH P 14456, FMNH P 14538

Tremacyllus cf. latifrons: FMNH P 14465, FMNH P 15254

Tremacyllus impressus: MACN-Pv 2434, MACN-Pv 2913, MACN-A 1377

Tremacyllus cf. impressus: MACN-Pv 16916

Specimens of *Tremacyllus* from Mendoza: IANIGLA-PV 26, IANIGLA-PV 440, IANIGLA-PV 564, IANIGLA-PV 553,

IANIGLA-PV 555, IANIGLA-PV 565/566, MACN-Pv 8497, MACN-Pv 8495, MACN-Pv 8494.

APPENDIX 2. List of specimens included in the lower cheek tooth analyses.

p2–m3 Analysis

Pachyrukhos moyani: FMNH P 12994, MACN-A 9958, MACN-A 330/335

Paedotherium bonaerense: FMNH P 14331, FMNH P 14330, MACN-Pv 5751, MACN-A 1670, MACN-A 1251/52, MACN-Pv 10513/10514, MACN-Pv 7253, MACN-Pv 17805, MACN-Pv 7732, MACN-Pv 7730, MACN-Pv 7729, MACN-Pv 7183, MACN-Pv 7413, MLP 91-IV-5-6, PVL 503

Paedotherium borrelloii: MLP 57-X-10-142

Paedotherium minor: MLP 29-IX-2-102, MLP 55-IV-28-30, MLP 60-VI-18-32, MLP 29-IX-2-103, MLP 29-IX-2-112

Paedotherium typicum: MACN-Pv 5883, MACN-Pv 6136, MACN-A 5755, MACN-Pv 16679, MACN-Pv 6436, MACN-Pv 17333, MLP 12-2703

Specimen of *Paedotherium* from Mendoza: IANIGLA-PV 23

Tremacyllus latifrons: FMNH P 14390, FMNH P 14456, FMNH P 14399

Tremacyllus impressus: MACN-Pv 2434

Tremacyllus cf. impressus: MACN-Pv 7207, MLP 57-X-10-86

Specimens of *Tremacyllus* from Mendoza: IANIGLA-PV 426, IANIGLA-PV 490, IANIGLA-PV 517, IANIGLA-PV 479, MACN-Pv 8502.

p3–m2 Analysis

Pachyrukhos moyani: FMNH P 12994, MACN-A 9958, MACN-A 330/335, MACN-A 259/261, MLP 12-1925/2759, MLP 12-2117/2125

Paedotherium bonaerense: FMNH P 14331, FMNH P 14330, MACN-Pv 5751, MACN-A 1670, MACN-A 1251/52, MACN-Pv 10513/10514, MACN-Pv 17883, MACN-Pv 7253, MACN-Pv 17805, MACN-Pv 7732, MACN-Pv 7730, MACN-Pv 7729, MACN-Pv 7183, MACN-Pv 7413, MACN-A 10269, MLP 91-IV-5-6, MLP 91-IV-5-56, PVL 503, PVL 2377

Paedotherium borrelloii: MLP 57-X-10-142, MLP 27-IX-20-38, MLP 57-X-10-114, MLP 57-X-10-43/52 (I), MLP 57-X-10-43/52 (II), MLP 57-X-10-82, MLP 57-X-10-82/85, MLP 65-VII-29-59/61

Paedotherium minor: MLP 29-IX-2-102, MLP 55-IV-28-30, MLP 60-VI-18-32, MLP 29-IX-2-103, MLP 29-IX-2-112, MLP 55-IV-28-31, MLP 60-VI-18-27, MLP 60-VI-18-34

Paedotherium aff. minor: MLP 29-X-10-88

Paedotherium typicum: MACN-Pv 5883, MACN-Pv 6136, MACN-A 5755, MACN-Pv 16679, MACN-Pv 6436, MACN-Pv 6031, MACN-Pv 15424, MACN-Pv 17333, MLP 12-2703, MLP 91-IV-5-62, MLP 91-IV-5-68

Specimens of *Paedotherium* from Mendoza: IANIGLA-PV 514, IANIGLA-PV 23

Tremacyllus latifrons: FMNH P 14390, FMNH P 14456, FMNH P 14399, FMNH P 14354, FMNH P 14359, FMNH P 1439, FMNH P 14400, FMNH P 15269

Tremacyllus cf. latifrons: FMNH P 14362, FMNH P 15255

Tremacyllus impressus: MACN-Pv 2434

Tremacyllus cf. impressus: MACN-Pv 7207, MLP 57-X-10-86

Specimens of *Tremacyllus* from Mendoza: IANIGLA-PV 457, IANIGLA-PV 496, IANIGLA-PV 510, IANIGLA-PV 549, IANIGLA-PV 554, IANIGLA-PV 555, IANIGLA-PV 196, IANIGLA-PV 445, IANIGLA-PV 448, IANIGLA-PV 426, IANIGLA-PV 490, IANIGLA-PV 517, IANIGLA-PV 479, MACN-Pv 8502